Title

The promiscuous development of an unconventional Qa1b-restricted T cell population.

Authors

Manoharan Valerio, Michael

Arana, Kathya

Guan, Jian

et al.

Publication Date

2023

DOI

10.3389/fimmu.2023.1250316

Peer reviewed

frontiers | Frontiers in Immunology

TYPE Original Research
PUBLISHED 31 October 2023
DOI 10.3389/fimmu.2023.1250316

OPEN ACCESS

EDITED BY
Nick Gascoigne,
National University of Singapore, Singapore

REVIEWED BY
Joanna Brzostek,
University of Freiburg, Germany
Ondrej Stepanek,
Institute of Molecular Genetics (ASCR), Czechia
Harvey Cantor,
Dana–Farber Cancer Institute, United States

*CORRESPONDENCE
Ellen A. Robey
erobey@berkeley.edu

†These authors have contributed equally to this work and share first authorship

RECEIVED 29 June 2023
ACCEPTED 06 October 2023
PUBLISHED 31 October 2023

CITATION
Manoharan Valerio M, Arana K, Guan J, Chan SW, Yang X, Kurd N, Lee A, Shastri N, Coscoy L and Robey EA (2023) The promiscuous development of an unconventional Qa1b-restricted T cell population.
Front. Immunol. 14:1250316.
doi: 10.3389/fimmu.2023.1250316

The promiscuous development of an unconventional Qa1b-restricted T cell population

Michael Manoharan Valerio[1†], Kathya Arana[1†], Jian Guan[2], Shiao Wei Chan[1], Xiaokun Yang[1], Nadia Kurd[1], Angus Lee[3], Nilabh Shastri[2], Laurent Coscoy[1] and Ellen A. Robey[1*]

[1]Division of Immunology and Molecular Medicine, Department of Molecular and Cell Biology, University of California Berkeley, Berkeley, CA, United States, [2]Department of Pathology, Johns Hopkins University School of Medicine, Baltimore, MD, United States, [3]Gene Targeting Facility Cancer Research Laboratory, University of California Berkeley, Berkeley, CA, United States

MHC-E restricted CD8 T cells show promise in vaccine settings, but their development and specificity remain poorly understood. Here we focus on a CD8 T cell population reactive to a self-peptide (FL9) bound to mouse MHC-E (Qa-1^b) that is presented in response to loss of the MHC I processing enzyme ERAAP, termed QFL T cells. We find that mature QFL thymocytes are predominantly CD8αβ+CD4-, show signs of agonist selection, and give rise to both CD8αα and CD8αβ intraepithelial lymphocytes (IEL), as well as memory phenotype CD8αβ T cells. QFL T cells require the MHC I subunit β-2 microglobulin (β2m), but do not require Qa1^b or classical MHC I for positive selection. However, QFL thymocytes do require Qa1^b for agonist selection and full functionality. Our data highlight the relaxed requirements for positive selection of an MHC-E restricted T cell population and suggest a CD8αβ+CD4- pathway for development of CD8αα IELs.

KEYWORDS

MHC-E, T cell development, unconventional T cells, non-classical MHC-1, IEL

Introduction

Thymic development of conventional CD8 T cells requires low affinity recognition of self-peptides bound to MHC I molecules expressed by cortical thymic epithelial cells and gives rise to naïve circulating CD8 T cells. Conventional CD8 T cells recognize peptides bound to classical MHC I (called MHC Ia) molecules, in contrast to unconventional T cell populations that recognize a diverse set of non-classical MHC I (called MHC Ib) (1, 2). MHC Ib molecules are structurally homologous to MHC Ia, and often associate with β2m, but are generally non-polymorphic, and can bind peptides or non-peptidic ligands (3). The two most prominent and well-studied examples of unconventional αβTCR-expressing T cells are mucosal associated invariant T cells (MAIT cells), that recognize vitamin B metabolites presented by MR1, and invariant natural killer T cells (iNKT cells), that recognize lipid metabolites presented by CD1d. MAIT cells and iNKT cells, like

conventional T cells, require their cognate MHC ligand to develop in the thymus (4, 5). However, unlike conventional T cells, which undergo positive selection by weak TCR signals, MAIT and iNKT cells undergo "agonist selection", an alternative thymic selection process in which strong TCR signals drive alternative differentiation programs instead of negative selection (6). In addition, MAIT and iNKT cells recognize self-ligands presented by thymic antigen presenting cells (APCs) of hematopoietic, rather than epithelial, origin (4, 5). The thymic development of T cells restricted to other MHC Ib molecules remains understudied (7–12).

While MHC Ib restricted T cells are relatively rare in circulation, they contribute substantially to the intraepithelial lymphocyte (IEL) compartment of the small intestine (13–15). αβTCR+ IEL are generally classified as either induced or natural IELs, which differ in their specificity and developmental pathways. Induced IELs, which express the CD8αβ heterodimer, are specific for classical MHC Ia molecules and are derived from conventional CD8 T cells following antigen encounter in the periphery (16, 17). On the other hand, natural IELs, which predominantly express the CD8αα homodimer, can recognize a variety of different MHC ligands and are programmed for an IEL fate by strong recogniton of self ligands in the thymus (18–20). Studies of natural IEL development have largely focused on populations of αβTCR+CD4-CD8- (double negative or DN) thymocytes, which can give rise to CD8αα IEL upon transfer into T cell deficient mice (21–25). However, it is unclear whether all natural IEL develop via an αβTCR+DN stage. Moreover, while it is known that many natural IEL require β2m, but not MHC Ia molecules, for their development (13–15, 18, 19), the specifity of IEL for particular MHC Ib molecules remains largely unknown. As a result, no studies to date have focused on the thymic development of IELs specific for defined MHC Ib molecules.

The MHC Ib molecule MHC-E (called Qa1 in mouse) is best known for its role in regulating NK cell responses; however, recent attention has focused on its function as a restricting MHC molecule for CD8 T cells (26, 27). In healthy cells, MHC-E molecules predominantly display a self-peptide derived from an MHC Ia leader peptide (called QDM peptide in mouse), which serves as a ligand for NK receptors and provides an inhibitory signal to NK cells and activated T cells (28, 29). However, under conditions of impaired MHC Ia presentation, such as deficiency in ERAAP (endoplasmic reticulum aminopeptidase associated with antigen processing) or TAP (transporter associated with antigen processing), $Qa1^b$ is loaded with an alternative set of peptides that can be recognized by CD8 T cells (10, 30–32). MHC-E restricted T cells responsive to TAP and ERAAP deficient cells have been proposed to play a role in monitoring defects in MHC Ia presentation induced by viral infection (33), transformation, or stress (31, 32). In addition, pathogen-specific MHC-E restricted CD8 T cells can be activated upon infection with a variety of viruses and bacteria (34–38). Recent studies of a CMV-vectored anti-HIV vaccine showed that MHC-E restricted CD8 T cells can produce responses that are extremely broad, with an unusually large proportion of the potential epitopes being targeted for recognition, and which provide strong immune protection (39, 40). Altogether, the ability of MHC-E restricted T cells to respond broadly to both microbial antigens and abnormal self, suggests an unusual mode of T cell recognition with significant therapeutic potential. However, our limited understanding of the specificity and development of MHC-E restricted CD8 T cells hampers our ability to harness these responses for therapeutic purposes.

Perhaps the best characterized example of an MHC-E restricted CD8 T cell response is QFL T cells, which recognize $Qa1^b$ loaded with a self-peptide FYAEATPML (FL9) derived from Fam49a/b proteins (31). QFL T cells were discovered as part of the mouse T cell response upon immunization of wild type mice with ERAAP deficient splenocytes. Interestingly, QFL T cells display hybrid characteristics of both conventional and unconventional T cells. Like conventional MHC Ia-restricted T cells, QFL T cells are found in the spleen and express the CD8αβ heterodimer. However, reminiscent of MAIT and iNKT cells, the majority use a semi-invariant TCR with a fixed TCRα and limited TCRβ usage (41). Splenic QFL T cells display an antigen experienced phenotype in wild type, unimmunized mice, reminiscent of conventional CD8 T cells that acquire a memory phenotype following homeostatic proliferation to self, termed "memory phenotype" or "virtual memory" T cells (42, 43). While QFL T cells can be detected using FL9-$Qa1^b$ tetramers (called QFL tetramers) in wild type and $Qa1^b$ deficient mice (31), their development in the thymus, and their contribution to the IEL compartment have not yet been examined.

Here we use both QFL tetramers and mice expressing rearranged QFL-specific αβTCR transgenes to probe the development of QFL T cells in wild type and MHC I deficient mice. QFL T cells can be readily detected in the spleen, thymus, and IEL compartment, with QFL T cells in the IEL compartment comprised of both CD8αα and CD8αβ phenotypes. Our data indicate that $Qa1^b$ expression, predominantly by hematopoietic cells, drives the agonist selection of QFL T cells in the thymus, leading to mature CD8+CD4- thymocytes that exhibit signs of strong TCR signals. However, QFL T cells also recognize an alternative MHC I ligand, which can allow for positive selection of QFL CD8SP thymocytes with a more conventional phenotype in the absence of $Qa1^b$. Our data highlight the promiscuous recognition and development of QFL T cells, confirm their hybrid conventional/unconventional characteristics, and suggest an alternative pathway for the development of natural IELs.

Results

Characterization of QFL T cells in wild type and TCR transgenic mice

To investigate the development of QFL specific T cells, we used tetramer enrichment of lymphocytes using $Qa1^b$ tetramers loaded with the FL9 peptide (31) (hereafter called QFL tetramers). To increase the specificity of detection, we co-stained using both the QFL tetramer and an antibody specific for Vα3.2, which recognizes the invariant TCRα chain used by the majority of QFL T cells (Supplementary Figures 1A, B; Figure 1A) (41). In this study, we focused on QFL $tetramer^+$ and $Vα3.2^+$ cells, hereafter called QFL T cells. The majority of QFL T cells in the thymus, spleen and small intestine (SI) intraepithelial lymphocyte (IEL) compartment of wild type mice were $CD8α^+$CD4- (Figure 1A). Interestingly, while mature

10.3389/fimmu.2023.1250316

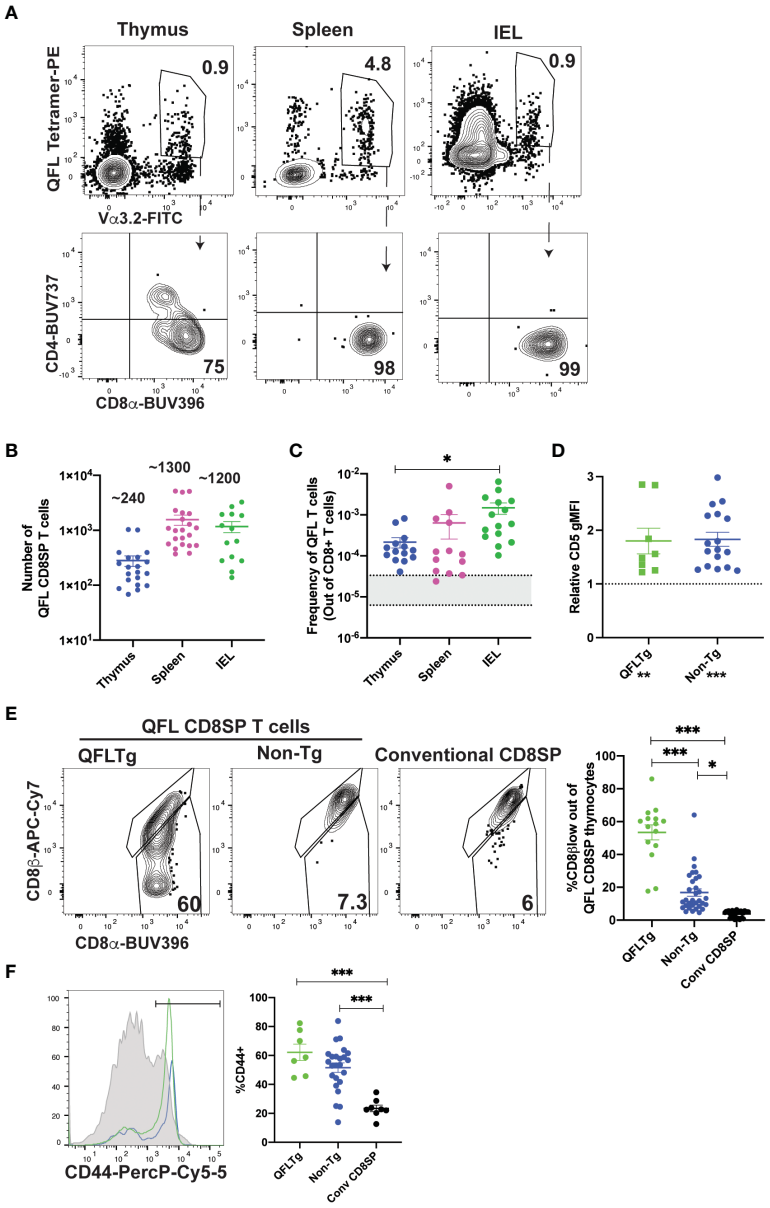

FIGURE 1
Characterization of QFL T cells in non-transgenic and transgenic mice. **(A-C)** QFL T cells were identified by flow cytometry from wild type mice. **(A)** Representative plots of QFL tetramer and Vα3.2 TCR expression from tetramer enriched thymocytes, tetramer enriched splenocytes, and unenriched small intestine intraepithelial lymphocytes (IEL). Splenocytes and IEL were gated for TCRβ+ cells. CD4 and CD8α expression on the indicated gated populations are shown below. **(B)** Absolute numbers of QFL CD8SP (single positive) T cells in the indicated compartments of wild type mice (Thymus n=20, IEL n=14, Spleen n=22) (Gated: QFL tetramer$^+$ Vα3.2$^+$ for thymus or TCRβ$^+$QFL tetramer$^+$ Vα3.2$^+$ for spleen and IEL). **(C)** Frequency of QFL CD8SP T cells out of total CD8SP T cells in the indicated compartments of wild type mice. For tetramer enriched samples, frequencies out of CD8 T cells were determined by back-calculating to the unenriched samples (Thymus n=14, IEL n=15, Spleen n=13). Greyed area represents the range of frequencies observed for naïve conventional CD8SP T cells (42, 44). **(D)** Relative CD5 expression (gMFI) of QFL CD8SP T cells from QFLTg mice (n=8) (Green) (Gated: QFL tetramer$^+$CD24$^-$CD8α$^+$CD4$^-$) and non-transgenic mice (n=17) (Blue) (tetramer enriched and gated: QFL tetramer$^+$ Vα3.2$^+$ CD8α$^+$CD4$^-$) normalized to the gMFI for conventional CD8SP (Dotted line) (Gated: CD4$^-$CD8α$^+$) analyzed in the same experiment. **(E)** Representative plots of CD8β and CD8α expression on mature QFL CD8SP thymocytes from QFL TCR transgenic mice (QFLTg) (Gated: QFL tetramer$^+$CD24$^-$CD8α$^+$CD4$^-$, as in Supplementary Figure 1), non-transgenic tetramer enriched (Gated: QFL tetramer$^+$ and Vα3.2$^+$ CD8α$^+$CD4$^-$) thymi. Conventional CD8SP (conv CD8SP) (Gated: CD8α$^+$CD4$^-$) from unenriched non-transgenic thymi are shown for comparison. Dot plots show compiled data from QFLTg (green) (n=15), non-transgenic QFL tetramer$^+$ thymocytes (blue)(n=32) and conventional CD8SP (black) (n=32). **(F)** Representative histogram of CD44 expression on QFL CD8SP T cells from splenocytes of QFLTg mice (Green), and non-transgenic mice (Blue) (tetramer enriched) (Gated: TCRβ$^+$B220$^-$QFL tetramer$^+$Vα3.2$^+$CD8α$^+$CD4$^-$), and conventional CD8SP T cells (Grey histogram). Dot plots show compiled data for QFL T cells from transgenic (n=7), non-transgenic (n=24) spleen and conventional CD8SP (conv CD8SP) (n=9). Error bars= Standard error of mean. Statistical analyses: One way ANOVA followed by Tukey's multiple comparison test was used for comparisons between experimental conditions **(C, E, F)**, symbols above dots. Students t test was used for comparisons between experimental samples **(D)**, symbol above dots. One sample t test was used for comparing experimental samples to the control used for normalization **(D)**, shown below experimental label. P values are *<0.05, ** <0.005, *** <0.0005. Comparisons that are not statistically significant are not marked by a symbol.

QFL T cells in thymus and spleen predominantly expressed the CD8αβ heterodimer, QFL T cells in the IEL compartment were a mixture of cells expressing CD8αα or CD8αβ (Supplementary Figures 1C–E). As previously reported (31), QFL T cells were relatively abundant in the spleen of wild type mice (~1300/spleen/mouse or 1/6000 CD8 T cells, Figures 1B, C). For comparison, a study of conventional CD8 T cell frequencies reported a range of 1/30,000 to 1/160,000 (42, 44). Additionally, a substantial number of QFL T cells were identified in the thymus and IEL compartment of the small intestine, with an average of 240 QFL T cells and 1,200 QFL T cells respectively (Figure 1B). The frequency of QFL T cells out of mature CD8 T cells was higher in the SI IEL compared to the thymus and spleen (Figure 1C), suggesting that they undergo selective recruitment and/or expansion in this compartment.

As a complimentary method to characterize QFL T cells, we developed a TCR transgenic mouse that expresses the semi-invariant QFL TCR α-and β-chain (Vα3.2Jα21, Vβ1Dβ1Jβ2-7) used by a predominant clone (41), henceforth referred to as QFLTg. As expected, mature (CD24-) thymocytes expressing the QFL TCR were predominantly CD8 single positive (SP) (Supplementary Figure 1A). DP thymocytes from transgenic mice expressed relatively low levels of the QFL TCR, while CD4SP thymocytes expressed moderately high levels of the TCR but remained mostly immature (CD24+) (Supplementary Figure 2A). To confirm that selection of the QFL CD8SP T cells in these mice was driven by the transgene encoded TCR, we examined expression of Vα2, which is expressed on ~10% of T cells in wild type mice and serves as a representative of endogenous TCRα expression. As expected, mature CD8SP in thymus and spleen of QFLTg mice had reduced expression of Vα2, whereas mature CD4SP has levels of Vα2 similar to wild type, confirming that CD8SP are mostly selected using the QFL TCR, whereas CD4SP are selected using endogenous TCRs (Supplementary Figures 2B, C). Importantly, the population defined as QFL CD8SP in this study (gated: QFL tetramer+Vα3.2+CD8+CD4-) was almost completely devoid of endogenous TCRα expression. These data validate the efficacy of our TCR transgenic system and confirms that QFL CD8SP in transgenic mice are selected by the transgene-encoded TCR.

We also used thymocytes and splenocytes from QFLTg mice to confirm the specificity of the QFL TCR for the FL9-Qa1^b complex. As expected, the majority of QFL tetramer+ thymocytes and splenocytes did not stain with tetramers in which Qa1^b was loaded with the predominant QDM peptide (Supplementary Figure 2D). The small population of QFL tetramer+ cells that did stain with the QDM tetramer also expressed the QDM/Qa1^b receptor NKG2A, an NK receptor that is also expressed by activated T cells. The co-staining of QDM tetramer and NKG2A suggests TCR independent binding of QDM tetramer on QFL T cells and serves as a positive control for QDM tetramer staining. These data confirm the specificity of the QFL TCR for the FL9/Qa1^b complex.

Previous studies showed that QFL T cells respond to a self-peptide presented by Qa1^b (31). In addition, splenic QFL T cells from wild type mice display an antigen experienced phenotype, suggesting that they may receive strong TCR signals during their development in the thymus. To test this notion, we examined expression of CD5, a marker which positively correlates with self-reactivity (45–48). As predicted, CD5 is elevated in QFL CD8SP thymocytes from QFLTg and non-transgenic mice compared to conventional CD8SP T cells (Figure 1D). In addition, QFL CD8SP thymocytes from non-transgenic mice showed slight but detectable downregulation of CD8β compared to conventional CD8SP T cells, whereas QFL CD8SP thymocytes from QFLTg mice showed more pronounced CD8β downregulation (Figure 1E). This modulation of CD8β expression has been associated with thymocyte self-reactivity and agonist selection (49, 50). QFL CD8SP thymocytes from QFLTg mice also showed elevated levels of several markers associated with agonist selection, such as the transcription factors PLZF (51, 52) and Tbet (Supplementary Figure 3). On the other hand, splenic, but not thymic, QFL CD8SP T cells express elevated levels of CD44, a marker associated with antigen experience (Figure 1F; Supplementary Figures 3A–C). In addition, QFL CD8SP thymocytes from QFLTg mice did not show detectable upregulation of PD1 or α4β7, markers that are expressed by a subset of thymic IEL precursors (Supplementary Figures 3A–C) (22). Taken together these data suggest that QFL T cells experience relatively strong TCR stimulation and undergo agonist selection during their development in the thymus.

QFL T cell development in absence of Qa1^b or classical MHC I

Some agonist selected T cell populations, such as regulatory T cells require a separate positive selection interaction prior to undergoing agonist selection (6). Previous reports that QFL T cells are detectable in the spleen of mice lacking Qa1^b, but undetectable in mice lacking β2m (31), a subunit of MHC I which is required for proper folding and surface expression of both classical MHC Ia and Qa1 (53), suggested the possibility that QFL T cells require positive selection on classical MHC Ia. To test this hypothesis, we generated K^{b}D^{b}KO mice and compared the number of QFL T cells in the thymus and spleen to that of WT and Qa1^{b}KO mice (Figure 2A; Supplemental Figures 4A, B). The QFL CD8SP thymocytes were slightly reduced in K^{b}D^{b}KO and Qa1^{b}KO relative to wild type mice, but were undetectable in β2mKO mice (Figure 2A). Similar results were obtained with QFLTg mice, with substantial numbers QFL thymocytes and splenocytes found in the absence of Qa1^b or K^{b}D^b, but not in the absence of β2m (Figure 2B). Importantly, the QFL CD8SP thymocytes and splenocytes from QFLTg, QFLTgQa1^{b}KO mice have negligible expression of endogenous Vα2 (Supplemental Figures 2B, C), confirming that these cells were positively selected using the QFL TCR. Classical MHC Ia D^b is the source for the QDM peptide that is bound to Qa1^b in ERAAP sufficient cells, raising the possibility that loss of D^b could indirectly impact QFL T cell development by altering the peptides displayed on Qa1^b. However, QFL CD8SP thymocytes and splenocytes were found in similar numbers in K^{b}KO, D^{b}KO, and K^{b}D^{b}KO mice, arguing against this possibility (Supplementary Figure 4C). Altogether, these data suggest that neither classical MHC Ia, nor Qa1^b, are required for QFL T cell positive selection, although both may contribute to the efficiency of the process. Interestingly, CD8SP T cells in spleens of K^{b}D^{b}KO mice

10.3389/fimmu.2023.1250316

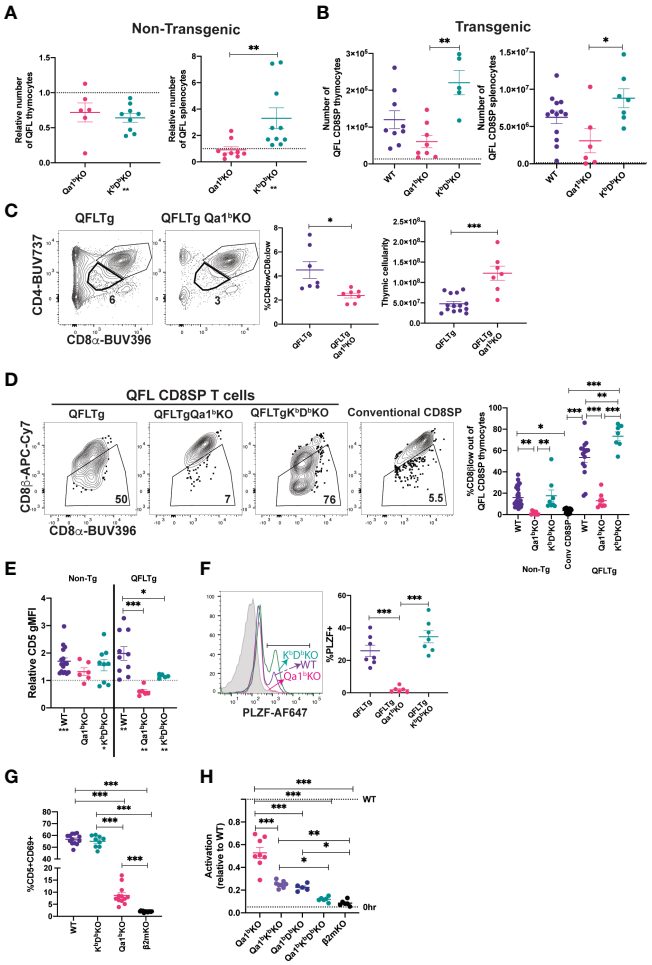

FIGURE 2
MHC requirements for QFL T cell development. **(A)** Relative number of QFL T cells in thymi (tetramer enriched and gated: QFL tetramer$^+$Vα3.2$^+$CD8α$^+$CD4$^-$) or spleen (tetramer enriched and gated: TCRβ$^+$QFL tetramer$^+$Vα3.2$^+$ CD8α$^+$CD4$^-$) of non-transgenic mice of the indicated genotype. To correct for variation in the efficiency of tetramer enrichment, data are normalized to the number of QFL T cells recovered from a wild type mouse analyzed in the same experiment (represented by dotted line)(Thymus Qa1^{b}KO n=6, K^{b}D^{b}KO n=9) (Spleen Qa1^{b}KO n=9, K^{b}D^{b}KO n=10. QFL T cells tetramer enriched from β2mKO mice are not shown as the value is 0. **(B)** Number of QFL CD8SP T cells in the thymi (Gated: QFL tetramer$^+$ CD24$^-$CD8α$^+$CD4$^-$)(WT n=9, Qa1^{b}KO n=8, K^{b}D^{b}KO n=5) or spleens (Gated: TCRβ$^+$QFL tetramer$^+$Vα3.2$^+$ CD8α$^+$CD4$^-$) (WT n=13, Qa1^{b}KO n=6, K^{b}D^{b}KO n=7) of QFLTg mice crossed to the indicated gene knock out strains. Dotted line represents the limit of detection which was based on β2mKO control (β2mKO controls were not considered for statistical analysis). **(C)** Representative plots of CD4 and CD8α expression on thymocytes from QFLTg and QFLTg Qa1^{b}KO mice. Dot plot shows compiled data for % of CD4lowCD8αlow in individual mice (Gated: live cells)(QFLTg n=7 and QFLTg Qa1^{b}KO=7). Panel to the right shows thymus cellularity from QFLTg (n=14) and QFLTg Qa1^{b}KO (n=7) mice. Each dot represents an individual mouse. **(D)** Representative plots of CD8β and CD8α expression on QFL CD8SP thymocytes (Gated: QFL tetramer$^+$CD24$^-$CD8α$^+$CD4$^-$) from QFLTg, QFLTg Qa1^{b}KO and QFLTg K^{b}D^{b}KO mice. Conventional CD8SP thymocytes from wild type mice (Gated : CD8α$^+$CD4$^-$) are shown for comparison. Graph shows % of CD8β low out of QFL CD8SP T cells in thymi of non-transgenic (WT n=26, Qa1^{b}KO n=8 and K^{b}D^{b}KO n=8), QFLTg (WT n=15, Qa1^{b}KO n=8 and K^{b}D^{b}KO n=7) mice or conventional CD8SP (Conv CD8SP) (Gated: CD8α$^+$CD4$^-$) from wild type mice(n=26). **(E)** CD5 expression on QFL CD8SP thymocytes from either non transgenic(tetramer enriched and gated: QFL tetramer$^+$Vα3.2$^+$CD8α$^+$CD4$^-$) (WT n=16, Qa1^{b}KO n=6 and K^{b}D^{b}KO n=9) or QFLTg (Gated: QFL tetramer$^+$CD24$^-$CD8α$^+$CD4$^-$) (WT n=10, Qa1^{b}KO n=6 and K^{b}D^{b}KO n=5) mice of the indicated genotypes. Graph shows gMFI of CD5 expression of QFL T cells normalized to the gMFI of conventional CD8SP thymocytes(Dotted line) (Gated: CD4$^-$CD8α$^+$) from wild type mice analyzed in the same experiment. **(F)** Representative histogram of PLZF expression in QFL CD8SP T cells (Gated: QFL tetramer$^+$CD24$^-$CD8α$^+$CD4$^-$) from QFLTg mice of the indicated genotypes (QFLTg n=7, QFLTg Qa1^{b}KO n=6 and QFLTgK^{b}D^{b}KO n=7). Grey histograms represent conventional CD8SP (Gated : CD8α$^+$CD4$^-$). **(G)** Pre-selection QFL thymocytes (preQFLTg) (from QFLTg β2mKO mice) were co-cultured with Bone Marrow Derived Dendritic cells (BMDC) from the indicated mouse strains. Compiled data of preQFLTg DP thymocyte (Gated: QFL tetramer$^+$Vα3.2$^+$CD4$^+$CD8α$^+$) expression of CD5 and CD69 after 24 hours of co-culture. Dot plots show compiled data from three experiments, with each dot representing a sample from an individual culture well (WT n=13, Qa1^{b}KO n=12, K^{b}D^{b}KO n=9 and β2mKO n=13). **(H)** preQFLTg thymocytes were co-cultured for 24Hrs with either parental (WT) DC2.4 cells or DC2.4 cells in which genes encoding the indicated MHC molecules were knocked out using CRISPR/Cas9 editing. The percentage of CD5$^+$CD69$^+$preQFLTg (Gated: QFL tetramer$^+$Vα3.2$^+$) thymocytes from each co-culture condition (Qa1^{b}KO, Qa1^{b}K^{b}KO, Qa1^{b}D^{b}KO, Qa1^{b}K^{b}D^{b}KO, and β2mKO) was normalized to the percentage of CD5$^+$CD69$^+$preQFLTg thymocytes co-cultured with WT DC2.4 cells, where WT=1 (Top dotted line). 0Hrs (Bottom dotted line) negative control represents the percentage of CD5$^+$CD69$^+$preQFLTg thymocytes before addition to co-culture. Dot plots show compiled data from three experiments, with each dot representing a sample from an individual culture well (Qa1^{b}KO n=8, Qa1^{b}K^{b}KO n=8, Qa1^{b}D^{b}KO n=5, Qa1^{b}K^{b}D^{b}KO n=5, and β2mKO n=6). Error bars= Standard error of mean. Statistical analysis: One way ANOVA followed by Tukey's multiple comparison test **(B–H)** (P values are * <0.05, ** <0.005, ***<0.0005) or Mann-Whitney test **(A, C)** (* <0.0332, ** <0.0021, *** <0.0002) were used for comparisons between experimental conditions (shown above dots. One sample t test was used for comparing experimental samples to the control used for normalization **(A, E)**: shown below experimental label) (P values are *<0.05, **<0.005, ***<0.0005). Comparisons that are not statistically significant are not marked by a symbol.

exhibit a higher frequency of Vα3.2$^+$ cells compared to WT or Qa1^{b}KO mice (Supplementary Figure 4D), indicating that this V segment is preferentially used by T cells reactive to MHC Ib molecules.

Because Qa1^b presents agonist FL9 peptide to QFL T cells, we hypothesized that expression of Qa1^b might lead to agonist and negative selection of QFL thymocytes. In support of this, DP thymocytes in QFLTg (Qa1^b sufficient) mice exhibit reduced cellularity and a "DP^{lo}" phenotype associated with strong TCR signals (19, 54–56) whereas QFLTg Qa1^{b}KO mice express normal levels of CD4 and CD8α (Figure 2C). In addition, QFL CD8SP thymocytes from Qa1^b sufficient, but not Qa1^{b}KO mice, displayed CD8β downregulation, PLZF expression, and elevated CD5 expression compared to conventional mature CD8SP thymocytes (Figures 2D-F). In contrast, in the absence of classical MHC I (K^{b}D^{b}KO mice) QFL CD8SP T cells showed strong downregulation of CD8β expression, maintained PLZF expression and showed a slight reduction in CD5 expression compared to WT mice (Figures 2D-F). In the periphery, QFL T cells lost their antigen experienced phenotype in absence of Qa1^b, but not in absence of classical MHC I (Supplemental Figure 4E). These data suggest that Qa1^b is required for agonist selection of QFL T cells, although positive selection of QFL T cells can be driven by an alternative MHC 1 molecule.

QFL T cells recognize an alternative ligand on Qa1^{b}KO APCs

To further explore the ligand-specificity of the QFL TCR we took advantage of the observation that MHC-naïve DP thymocytes are highly sensitive to *in vitro* TCR stimulation (57, 58). We examined expression of activation markers on pre-selection QFLTg (preQFLTg) thymocytes from a β2mKO background after co-culture with bone marrow derived dendritic cells (BMDC) isolated from mice lacking either Qa1^b, K^{b}D^b or β2m. PreQFLTg thymocytes showed stronger upregulation of the activation markers CD69 and CD5 upon 24-hour co-culture with WT and K^{b}D^{b}KO, compared to Qa1^{b}KO, BMDC (Figure 2G; Supplementary Figure 5A). This is consistent with the hypothesis that Qa1^b is the primary MHC ligand for the QFL TCR. Interestingly, preQFLTg thymocytes showed a modest activation when co-cultured with Qa1^{b}KO BMDCs; this activation was significantly more compared to co-culture with β2mKO BMDCs (Figure 2G). A similar pattern of reactivity was observed when preQFLTg were cultured in thymic slices derived from WT, Qa1^{b}KO and β2mKO mice (Supplementary Figures 5B, C). This is consistent with the development of QFL T cells in Qa1^{b}KO mice, and suggests that the QFL TCR is cross-reactive with an alternative β2m-utilizing molecule.

To further explore the specificity of the QFL TCR for MHC 1 molecules, we used the DC-like cell line DC2.4 as a stimulator cell for preQFLTg thymocytes (Figure 2H; Supplementary Figure 5D). The response of preQFLTg thymocytes to DC2.4 cells was abolished by CRISPR/Cas9 mediated gene knock out of β2m and partially reduced by loss of Qa1^b, paralleling the results from stimulation with BMDC, and pointing to the recognition of an alternative MHC-1 ligand in this system (Figures 2G, H). Interestingly, triple KO of Qa1^b, K^b, and D^b in DC2.4 cells reduced activation close to background levels, whereas double knock out of Qa1^b with either K^b, or D^b led to stimulation that was intermediate between the triple KO and Qa1^b KO cell lines. Together these data suggest that classical MHC-1 molecules may contribute to the positive selection of QFL T cells in Qa1^{b}KO mice.

QFL T cell selection by hematopoietic and non-hematopoietic cells

While conventional αβT cells undergo positive selection by recognition of MHC molecules on thymic epithelial cells, MAIT cells and iNKT cells undergo selection via interactions with hematopoietic cells (4, 5). To investigate the cell type requirements for selection of QFL T cells, we generated reciprocal bone marrow chimeric mice in which either the donor cells or the host cells are β2mKO, and therefore lack surface expression of Qa1, as well as the classical MHC I molecules H2-D, H2-K (Supplementary Figure 6). Interestingly, comparable numbers of QFL T cells were found in the thymus and spleen of the β2mKO>WT and WT>β2mKO chimeric mice (Supplementary Figures 6B, C), implying that QFL T cell development could occur efficiently on either non-hematopoietic or hematopoietic cells. To confirm these results, we generated reciprocal β2mKO chimeras using donor cells that expressed the QFL TCR transgene (Figure 3A). While there was some reduction in QFL T cell number in the thymus of β2mKO>WT compared to WT>β2mKO and wild type control chimeras (Figure 3B), similar numbers of QFL T cells were found in the spleen (Figure 3C). Thus, QFL T cell development is not strictly dependent on either non-hematopoietic or hematopoietic expression of MHC I.

We also examined whether QFL T cells that are selected exclusively by hematopoietic or non-hematopoietic cells retained their agonist selected phenotype. QFL thymocytes exhibited comparable CD8β downregulation but decreased PLZF expression when MHC I was restricted to non-hematopoietic cells (Figures 3D, E; Supplementary Figure 6D). Similarly, expression of CD5 was decreased when MHC I was restricted to non-hematopoietic cells (Figure 3F; Supplementary Figure 6E). In the periphery, QFL T cells in chimeric mice that lacked MHC I on hematopoietic cells did not display elevated expression of CD44 (Figure 3G; Supplementary Figure 6F). Overall, the thymic phenotype of QFL T cells in β2mKO>WT chimeras is similar, but not identical, to that observed in Qa1^{b}KO mice (Figures 2D–F). These data suggest that Qa1^b on both hematopoietic and non-hematopoietic cells contribute to agonist selection, with hematopoietic cells playing the predominant role.

Impact of agonist selection on QFL T cell function

To test how agonist selection impacts the functionality of QFL T cells, we compared QFL T cells that arose in the presence or absence of Qa1^b for their ability to respond *in-vitro* to ERAAPKO

10.3389/fimmu.2023.1250316

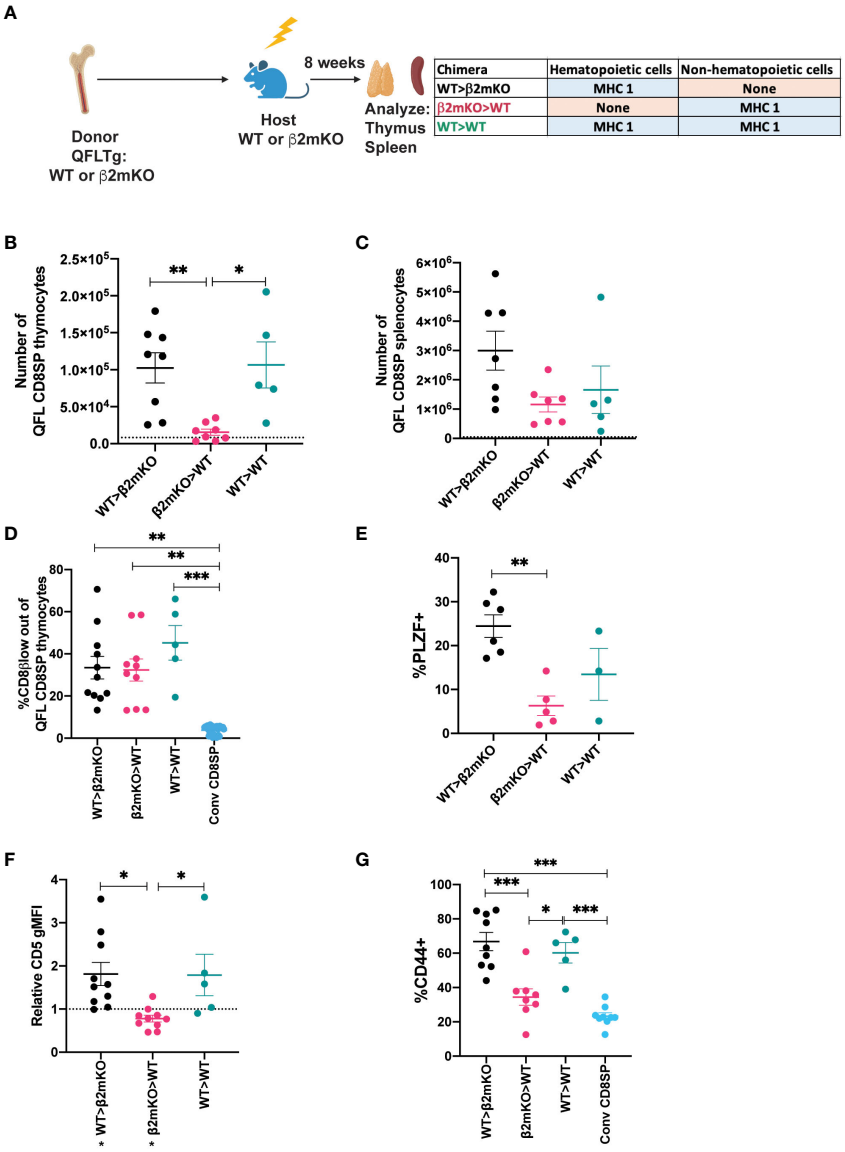

FIGURE 3
Requirement for hematopoietic versus non-hematopoietic cell MHC I expression for QFL thymic selection. **(A)** Diagram of experimental design. QFLTg or QFLTg β2mKO mice were used as bone marrow donors to reconstitute irradiated β2mKO or wild type hosts in order to restrict MHC I expression to hematopoietic or non-hematopoietic cells. **(B, C)** Absolute numbers of QFL CD8SP T cells in the indicated chimeric mice in **(B)** Thymus (Gated: QFL tetramer$^+$CD24$^-$CD8α$^+$CD4$^-$) (WT>β2mKO (black) n=8, β2mKO>WT (magenta) n=8, WT>WT (teal) n=5) and **(C)** Spleens (Gated: TCRβ$^+$QFL tetramer$^+$Vα3.2$^+$CD8α$^+$CD4$^-$)(WT>β2mKO n=7, β2mKO>WT n=7, WT>WT n=5). Dotted line represents the limit of detection which corresponds to the small number of events that appear in the QFLCD8SP T cell gate in β2mKO>β2mKO mice. **(D)** Downregulation of CD8β on QFL CD8SP thymocytes (Gated: QFL tetramer$^+$CD24$^-$CD8α$^+$CD4$^-$) of the indicated chimeric mice (WT>β2mKO n=11, β2mKO>WT n=10, WT>WT n=6). Conventional CD8SP (conv CD8SP, Gated: CD8α$^+$CD4-) (light blue) (n=11) from unenriched non-transgenic mice are shown for comparison. **(E)** Quantification of PLZF expression in QFL CD8SP thymocytes from the indicated chimeric (WT>β2mKO n=6, β2mKO>WT n=5, WT>WT n=3). **(F)** Relative CD5 expression on QFL CD8SP thymocytes of the indicated chimeric mice normalized to CD5 expression (gMFI) of conventional CD8SP (Dotted line) (Gated: CD4$^-$CD8α$^+$) thymocytes from wild type mice analyzed in the same experiment. (WT>β2mKO n=11, β2mKO>WT n=10, WT>WT n=5). **(G)** CD44 expression on QFL CD8SP T cells (Gated: TCRβ$^+$QFL tetramer$^+$Vα3.2$^+$CD8α$^+$CD4$^-$) from: WT>β2mKO, β2mKO>WT, WT>WT chimeric spleens. CD44 expression on conventional CD8SP (Conv CD8SP) (Gated: TCRβ$^+$CD8α$^+$CD4$^-$) from wild type mice is shown for comparison. (WT>β2mKO n=9, β2mKO>WT n=8, WT>WT n=5). Error bars= Standard error of mean. Statistical analysis: One way ANOVA followed by Tukey's multiple comparison test **(B–G)** were used for comparisons between experimental conditions (shown above dots). One-sample t test was used for comparing experimental samples to the control used for normalization **(F)**: shown below experimental label (P values are *<0.05, ** <0.005, *** <0.0005). Comparisons that are not statistically significant are not marked by a symbol.

splenocytes. QFL T cells from QFLTg showed extensive upregulation of activation markers and increased proliferation in response to stimulation compared to QFL T cells from QFLTg Qa1^{b}KO mice (Figures 4A, B). This implies that agonist selection on Qa1^b led to greater functional responsiveness, which could reflect greater functionality on a per cell basis, or an increased frequency of functional cells within the population. Since agonist selection partially correlates with selection on hematopoietic cells (Figure 3; Supplementary Figure 6), we also examined QFL splenocytes from reciprocal β2mKO and wild type bone marrow chimeric mice as a

10.3389/fimmu.2023.1250316

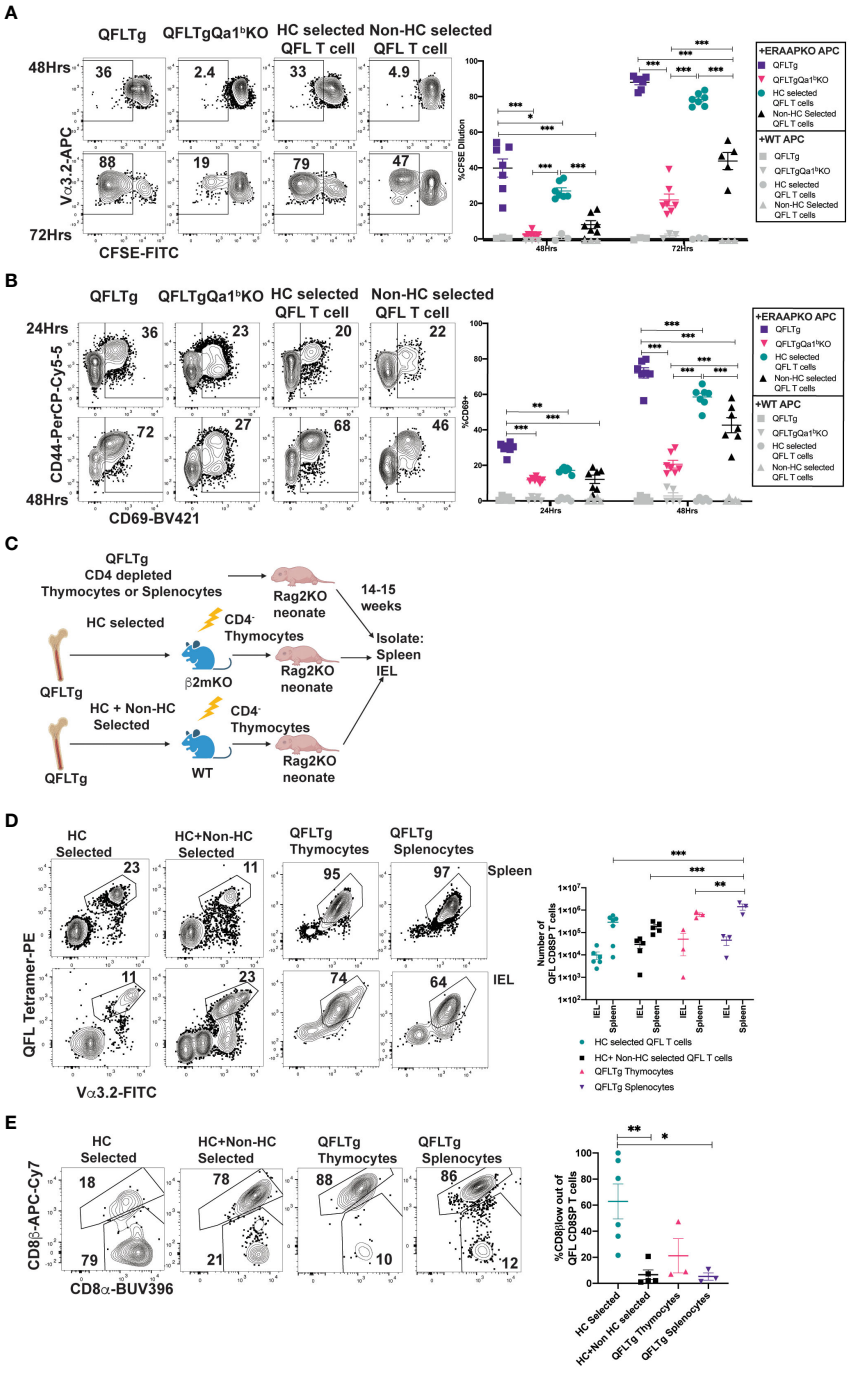

FIGURE 4
Agonist selected QFL T cells respond rapidly to antigen exposure and home to the IEL compartment. **(A, B)** QFL CD8SP T cells from QFLTg, QFLTgQa1^{b}KO, QFLTg>β2mKO [Hematopoietic cell (HC) Selected] and QFLTgβ2mKO>WT (non-HC selected) spleens were labeled with CFSE and co-cultured with splenocytes from WT or ERAAPKO mice, and analyzed after 24, 48, or 72 hours of co-culture. Representative plots and quantification of CFSE dilution **(A)** or CD69 surface expression **(B)** on QFL CD8SP T cells (Gated: TCRβ^{+}B220^{-}QFL tetramer^{+} Vα3.2^{+}CD8α^{+}). Compiled data of two experiment (n=7 for all conditions). **(C)** Experimental design: Bone marrow chimeric mice were generated using QFLTg bone marrow donors and hosts deficient or sufficient for β2m (as in Figure 3A), and CD4-depleted thymocytes from the chimeric mice were injected into Rag2KO neonates. For comparison, CD4-depleted QFLTg thymocytes or splenocytes were transferred into Rag2KO neonates. The spleen and small intestinal IEL compartments were analyzed 14-15 weeks post injection. **(D)** Representative plots of QFL tetramer and Vα3.2 TCR expression from spleen (HC selected n=7, HC+nonHC selected n=5, QFLTg thymocytes n=3, and QFLTg splenocytes n=3) or IEL (HC selected n=6, HC+nonHC selected n=5, QFLTg thymocytes n=3, and QFLTg splenocytes n=3) of the indicated transferred Rag2KO mice (Gated: Donor^{+}TCRβ^{+}). Compiled data show the number of QFL CD8SP T cells (Gated: QFL tetramer^{+}Vα3.2^{+}CD8α^{+}) recovered from each sample. Each dot represents an individual mouse **(E)** Representative plots of surface expression of CD8α and CD8β on QFL CD8SP T cells (Gated: TCRβ^{+}QFL tetramer^{+}Vα3.2^{+}CD8α^{+}) isolated from the IEL compartment of the indicated transferred Rag2KO mice (HC selected n=6, HC+nonHC selected n=5, QFLTg thymocytes n=3, and QFLTg splenocytes n=3). Compiled data shows %CD8β low out of QFL CD8SP IEL T cells recovered from indicated transferred Rag2KO mice. Each dot represents an individual mouse. Error bars= Standard error of mean. Statistical analyses: Two-way ANOVA followed by Tukey's multiple comparison test comparing samples to each other in their respective time point **(A, B)** or organ group **(D)**. One way ANOVA followed by Tukey multiple comparison comparing each sample to each other **(E)**. P values are *<0.05, **P<0.005, ***<0.0005. Comparisons that are not statistically significant are not marked by a symbol.

further test of the impact of agonist selection on function. QFL T cells from QFLTg>β2mKO mice (Hematopoietic cell (HC) selected) responded more robustly to ERAAPKO APCs compared to cells from QFLTg β2mKO>WT mice (non- HC selected) (Figures 4A, B). Thus, QFL T cells that develop in the absence of Qa1^b, or in the absence of hematopoietically expressed MHC I, exhibit reduced functionality.

QFL thymocytes and splenocytes can populate the intestinal epithelial compartment

QFL thymocytes display an agonist selected phenotype that is enhanced by hematopoietic expression of MHC I. Given that agonist selection in the thymus can give rise to natural intraepithelial lymphocytes, we considered that QFL thymocytes might represent a population of IEL precursors. To test this idea, we injected Rag2KO neonatal mice with CD4-depleted QFL thymocytes from HC-only selected (QFLTg>β2mKO) or both HC and non-HC selected (QFLTg>WT) chimeric mice (Figure 4C). For comparison, we also injected Rag2KO neonatal mice with CD4-depleted thymocytes or splenocytes from intact QFLTg mice. QFL T cells were found in similar numbers in the spleen and IEL compartment of the SI for all 4 donor populations (Figure 4D). Interestingly, IEL T cells derived from HC-only selected QFL thymocytes showed more pronounced downregulation of CD8β (~50%) when compared to IEL T cells derived from HC+ non-HC selected QFL T cells (~10%) (Figure 4E). Altogether, these data indicate that both QFL thymocytes and splenocytes contain IEL precursors, and that selection by hematopoietic cells favors CD8β downregulation in QFL IELs.

Discussion

Most studies of unconventional T cells have focused on 2 prominent populations, MAIT (MR1-restricted) and iNKT (CD1d restricted) cells, and much less is known about the development of T cells restricted to other MHC Ib molecules. Moreover, while it is known that non classical MHC molecules contribute substantially to the CD8αα natural IEL compartment (13, 15, 54), and there is evidence that thymic mature CD4-CD8- (DN) cells contain IEL precursors (21, 22, 25, 59), it is unclear whether all natural IEL develop via a mature DN pathway. Here we have used both QFL TCR transgenic mice and FL9-Qa1^b tetramer staining of non-transgenic mice to investigate the development of a population of self-reactive Qa1^b restricted cells known as QFL T cells. QFL T cells are found in circulation as both naïve and memory phenotype CD8αβ T cells, and in the IEL compartment as both CD8αα and CD8αβ cells, whereas mature QFL thymocytes are predominantly CD8αβ+CD4- and show signs of agonist selection. QFL T cells have a more relaxed requirement for positive selection compared to conventional CD8 T cells, requiring β2m on either hematopoietic or non-hematopoietic cells, but neither the restricting molecule Qa1^b, nor MHC Ia for positive selection. However, QFL thymocytes do require Qa1^b for agonist selection and full functionality. Our data highlight the promiscuous requirements for positive selection of a Qa1 restricted T cell population and identify an alternative CD8αβ+CD4- pathway for development of CD8αα IELs.

The flexible thymic development of QFL T cells parallels their ability to give rise to T cells with both conventional and unconventional properties. Unconventional MAIT and iNKT cells require selection by their restricting MHC molecules on hematopoietic cells, giving rise to T cells that migrate directly to tissues and exhibit preformed effector program. On the other hand, conventional CD8 T cells require selection by their restricting MHC Ia molecules on thymic epithelial cells, producing circulating naïve T cells that lack effector programing. QFL T cells appear to have the option to develop by either of these pathways, with selection by Qa1^b on hematopoietic cells leading to a more unconventional phenotype, and selection via an alternative MHC I ligand giving rise to T cells that resemble conventional CD8 T cells. Interestingly, the ability to be selected on either hematopoietic or non-hematopoietic cells in the thymus has been reported both for another Qa1 restricted T cell population (9), as well as a T cell population restricted to the MHC Ib molecule H2-M3 (8). While the M3 restricted cells required M3 expression for thymic selection, hematopoietic selection led to T cells with more unconventional functional properties compared to non-hematopoietic selection. Thus, a flexible pattern of thymic selection leading to alternative functional programs may be a general feature of T cell reactive to Qa1 and H2-M3.

The IEL compartment harbors 2 distinct types of αβTCR+CD8+ T cells: "induced" CD8αβ T cells that are derived from conventional CD8 T cells following encounter with foreign antigen and differentiation into tissue resident memory T cells, and "natural" CD8αα IEL that are directed into an IEL program in the thymus due to their high self-reactivity (16, 17). The observation that the same TCR clone can give rise to both types of IEL blurs the distinction between these two types of cells. Previous studies of natural IEL development have suggested a pathway in which some DP thymocytes that receive strong TCR signals escape clonal deletion by downregulating CD4 and CD8 to give rise to mature CD4-CD8- IEL precursors (IELp), that can eventually migrate to the gut and upregulate CD8αα (17, 22). Our data are consistent with an alternative pathway for IEL development in which agonist selection leads to a mature CD8αβ+CD4- thymic IELp. While the ability of CD4-depleted thymocytes to repopulate the IEL compartment of Rag2KO mice does not rule out a contribution from CD4-CD8α- precursors, the absence of detectable CD4-CD8α-QFL thymocytes in non-transgenic mice, as well as the agonist phenotype of thymic QFL CD8SP, strongly suggests that the CD4-CD8αβ cells are the relevant thymic precursor population. Moreover, the partial downregulation of CD8β observed on mature QFL thymocytes and on some QFL IEL T cells, suggests that CD8β expression may be unstable in QFL cells, leading to partial or full downregulation once they arrive in the IEL compartment. The suggestion is also consistent with the observation that splenic QFL T cells, which are uniformly CD4-CD8αβ, can give rise to IELs expressing intermediate levels of CD8β upon transfer into Rag2KO recipients. Altogether, these data are in line with earlier studies of thymocytes agonist selection in organ culture that also implicated mature CD8SP as a thymic precursor to natural IEL (49,

50). A detailed understanding of the developmental pathways and signals involved in QFL IEL T cell development awaits further investigation.

Our data, together with published observations, support the notion that MHC-E restricted CD8 T cells are generally cross-reactive. Using an *in vitro* stimulation assay with pre-selection QFL thymocytes, which reads out relatively weak TCR signals compatible with positive selection (57, 58), we found that QFL thymocytes can respond to Qa1^{b}KO APCs, but not to APC lacking Qa1^b as well as both K^b and D^b classical MHC1a molecules. Thus, cross-reactivity to classical MHC-1 molecules may account for the positive selection of QFL thymocytes in the absence of Qa1^b. In addition, another Qa1^b restricted clone was shown to cross react with an MHC Ia molecule (60), although it was dependent on Qa1^b for its positive selection (9). The MHC-E restricted response to a CMV-vectored HIV vaccine showed extremely broad reactivity, with detectable responses to 4 epitopes for every 100 amino acids (61). In this regard, it is intriguing that QFL T cells show strong preferential use of Vα3.2 (encoded by TRAV9N/D-3) (41). Vα3.2 is preferentially used by CD8 T cells compared to CD4 T cells (62) and has been suggested to be inherently reactive to MHC I (63). In addition, Vα3.2 is enriched in a subset of natural IELs (22), and is used by another Qa1^b-restricted CD8 T cell clone (9). Moreover, we found that the frequency of Vα3.2+ CD8 T cells is substantially increased in K^{b}D^{b}KO mice (Supplementary Figure 4D). Altogether, these observations suggest that Vα3.2 may work together with Qa1^b, and perhaps other non-classical MHC I molecules, to generate self-reactive T cells with a propensity to give rise to memory phenotype and natural IEL T cells.

If MHC-E reactive CD8 T cells are inherently cross-reactive, how do they escape negative selection in the thymus? While thymocyte intrinsic mechanisms, such as downregulation of CD4 and CD8 may contribute (56), it is interesting to consider how properties of the MHC molecules may also play a role. In particular, MHC-E molecules tend to be expressed at lower levels on the cell surface compared to MHC Ia molecules (9, 64, 65), a property that may be linked to their atypical peptide presentation pathway (66, 67) and/or low surface stability (64). In addition, MHC-E molecules predominantly express a single self-peptide derived from MHC Ia leader peptides (68, 69), and may not present a large array of self-peptides in healthy cells. Indeed, it has been proposed that MHC-E molecules may monitor alterations in the MHC Ia peptide presentation pathway that occur upon viral infection or cellular transformation (10, 31, 33), changes which may be mimicked by conditions of cellular stress. According to this notion, MHC-E restricted T cells may undergo rare or transient encounters with high affinity self-peptide-MHC-E complexes on stressed cells during their development in the thymus, allowing them to experience agonist selection signals while avoiding negative selection.

Methods

Mice

B6 (C57BL/6), B6 Ly5.1 (B6.SJL-*Ptprca Pepcb*/BoyJ) and Rag2-/- (B6(Cg)-Rag2tm1.1Cgn/J) mice were from Jackson Labs. B2M-/- (B6.129-B2mtm1Jae N12) mice were from Taconic. Qa1^{b}KO mice (70) were obtained from the Shastri lab. TCR transgenic mice specific for FL9-Qa1^b (QFL) and H-2K1/H-2D1-/- (K^{b}D^{b}KO) mice were generated in our lab (described below). All mice were bred in the UC Berkeley animal facility and all procedures were approved by the Animal Care and Use Committee (ACUC) of the University of California.

Generation of the QFLTg mouse

The TCR alpha and beta chain sequences from the QFL specific BEKo8z hybridoma (31, 41) were cloned and amplified from the genomic DNA of the BeKoz Hybridoma. The TRAV9N/D-3 TCR alpha chain was cloned with the forward primer (5' AAAACCCGGGCCAAGGCTCAGCCATGCTCCTGG) with an added XmaI cutting site at 5' end of the DNA sequence and a reverse primer for TRAJ21 (5' AAAAGCGGCCGCATA CAACATTGGACAAGGATCCAAGCTAAAGAGAACTC) with an added Not1 cutting site at the 5' end of the DNA sequence. The TCR beta chain was cloned with the forward primer (5' AAAACTCGAGCCCGTCTGGAGCCTGATTCCA) with and added Xho1 cutting site at the 5' end of the DNA and a reverse primer for TRBJ2-7 (5' AAAACCGCGGGGGACCCAG GAATTTGGGTGGA) with a SacII cutting site flanking the 5' end of the DNA sequence. The cloned TCR alpha chain was cloned into pTα cassette vector by inserting it between the Xmal and Not1 sites, while the TCR beta chains were cloned into pTβ cassette vector in between the Xhol and SacII sites (71). The ampicillin resistance gene was removed from pTα and pTβ cassette by EarI enzyme digest. The QFL transgenic mice were generated on the B6 background in the Cancer Research Laboratory Gene Targeting Facility at UC Berkeley under standard procedures. The QFL mice were maintained on the B6 background and bred once with B6 5.1 mice to generate (QFLTgxB65.1/2) background mice for use in experiments. Founder mice were identified by flow cytometry and PCR genotyping of tail genomic DNA using primers mentioned above.

Generation of K^{b}D^{b}KO mice

K^{b}D^{b}KO were generated by the Gene Targeting Facility at UC Berkeley using Cas9/CRISPR-mediated gene targeting. The H-2K1 gene was targeted using an sgRNA (5' GTACATGGA AGTCGGCTACG 3') that aligned with the sense strand and the H-2D1 gene was targeted using an sgRNA (5' AGATGTACCG GGGCTCCTCG 3') that aligned with the antisense strand. Wild-type C57BL/6J mice were originally obtained from the Jackson Laboratories. Zygotes were obtained from super ovulated C57BL/6J females for CRISPR/Cas9 targeting knockout experiment. In brief, CRISPR mix (i.e., Cas9 protein and sgRNAs) was introduced to zygotes by electroporation as previously described (72).The embryos were then transferred to 0.5dpc pseudo pregnant females (CD-1, Charles River Laboratories) with oviduct transfer. When the pups were born, tails samples were collected for DNA extraction

and genotyping. The resulting founder mice were identified by flow cytometry. The H-2K1 gene had a 2bp deletion (5' TGCCTGGGCTTTCTGTGTCTCCCGCTCCCAATACTCGGGC CCCTCCTGCTCCATCCACCGC GCCCGCGGCTCATATCTCG GATTCTCCGCGTCGCTGTCGAAGCGCACGAACTCCGTG TCGTCCACGT—CCGACTTCCATGTACCGGGGCTCCC CGAGGCCGGGCCGGGACACGGCGGTGACGAAAT ACCTCAA 3') where the sgRNA targeted. The H-2D1 gene had a 15bp deletion where the sgRNA targeted (5' CCGTNGGGT CGTTCTGTTCCAAACCTCGGACTTGGGACCCGG GACGTCAGCGTCCCTGTGTCGGGAAGTGGAG GGGCCTGACCTCCCACGCGGGGTCACTCACCGCCC GCGCTCTGGTTGTAGTAACCNAGCAGGTTCCT CAGGCTCACTCGGAACCACTGCTCTTGGGCCTTGGNTTTC TGTGTTTCCCGCTCCCAATACTCCGGCCCCTCCT GCTCCATCCACGGCGCCCGCGGCTCATATCTCG GATTCTCCGCGTCGCTTTCGAAACGCACGAACTCCTTGTT GTCCACATAGCCAACAGAGATGTACCGGGGC————— CGGGACACGGCGGTCTCGAAATACCGCATCGAG TGTGGGCCTGGGGACGGCGCGCGGTGAGACC CCGACCTCCTCACCAAACCCCGGGCGGCTGCGCA CGCCGGGAGGGGATCTGGGCGCGGGGCTCAGG TGGAGAAGGGGCGGAGGGTCCGNGGGGGCGACGA 3').

Preparation of cell suspension

Thymi, and spleens were mechanically dissociated in FACS buffer (0.5% BSA in PBS) or complete RPMI (10% FBS) to generate single-cell suspensions that were then passed through a 70µm filter. Intraepithelial lymphocytes (IELs) were isolated from the small intestine as previously described (73). Briefly, small intestine was cut to 1cm pieces and washed with cold CMF. Tissue pieces were allowed to settle and CMF was poured off. The tissue was then digested with DTE solution for 30 min at 37C in a 50mL conical tube. Tissue pieces were centrifuged at 1,500rpm for 5 min at 4C. Supernatant was collected and centrifuged at 1,500rpm for 5min at 4C. Lymphocytes were isolated by percoll separation utilizing 40% and 80% percoll (22). The percoll solution was centrifuged at 2000rpm with no brake for 20 min at room temperature. Lymphocyte layer was then washed with PBS and collected. Splenocytes were then RBC lysed using ACK lysis buffer (0.15M NH4Cl, 1mM KHCO3, 0.1mM Na2EDTA) for 5 minutes at room temperature.

Staining for flow cytometry

Thymi, spleens, and IELs were stained in 2.4G2 supernatant for 30 minutes at 4°C with the following antibodies: (BD Biosciences) CD4 (RM4-4), CD8α (53-6.7), CD5 (53-7.3), PLZF (R17-809), (Biolegend) TCRβ (H57-597), CD8β (YTS156.7.7), B220 (RA3-6B2), Vα3.2 (RR3-16), CD45.2 (104), T-bet (4B10), (Invitrogen) CD8β (H35-17.2), CD24 (M1/69), integrin α4β7 (DATK32), CD69 (H1.2F3) (Tonbo) CD44 (IM7), and CD45.1 (A20). Cells were then washed in PBS and stained in Ghost Dye Violet 510 as described above. For intracellular staining, cells were fixed and permeabilized using the eBioscience FoxP3/ Transcription Factor Staining Buffer Set (ThermoFisher) according to manufacturer's instructions. Biotinylated peptide-MHC monomers were obtained from the NIH Tetramer Facility (Atlanta, GA). Tetramers were assembled by conjugating the biotin-labeled monomers with PE-labeled streptavidin (Agilent, #PJRS27-1) according to NIH Tetramer Facility protocols. Cell numbers were calculated using AccuCheck Counting Beads for count and pipetting accuracy (Life Technologies #PCB100) according to manufacturer's instructions. All antibodies were from BD Biosciences, Biolegend, Invitrogen, or Tonbo Biosciences. Samples were processed using a Fortessa X20 (BD Biosciences) and analyzed using FlowJo software. For defining CD8α+CD8βlow thymocyte population, we adjusted the gate based on wild type controls samples analyzed in parallel to experimental samples, such that 5-6% of the wild type CD8SP cells were CD8βlow. This gate was then applied to our experimental samples (as shown in Figure 1E). Similarly, the CD8α+CD8βlow gate in the IEL population was placed based on wild type samples run in parallel and then applied to experimental samples (Supplementary Figure 1C).

Tetramer enrichment

Single-cell suspensions of thymi and spleens were generated as described above. Cells were incubated in 50nM Datsatinib (Sigma Aldrich, CDS023389-25MG) for 30 minutes at 37°C and then stained with tetramer in 2.4G2 supernatant for 1 hour at room temperature. After staining, cells were washed and incubated with Anti-PE MicroBeads (Miltenyi Biotec, #130-048-801) in MACS buffer (0.5% BSA) for 30 minutes at 4°C. Cells were then positively enriched for tetramer+ T cells using a magnetic column (Miltenyi Biotec.) according to manufacturer's instructions and washed before extracellular staining.

Bone marrow dendritic cell culture *in vitro* stimulation

Bone marrow cells were harvested as described above and RBC lysed using ACK lysis buffer (0.15M NH4Cl, 1mM KHCO3, 0.1mM Na2EDTA) for 5 minutes at room temperature. Bone marrow cells were resuspended in cRPMI and seeded at 5 x 10^6 cells per milliliter in 24 well plates. Cells were supplemented with GM-CSF (Peprotech, #315-03-20UG) until day 4 and adhering cells were harvested on day 6 using EDTA. 6 x 10^5 CD11c+MHC-II+ bone marrow cells per milliliter were seeded in 24 well plates. Preselection QFL thymocytes were generated by crossing QFL TCR transgenic mice onto a non-selecting, MHC-I deficient background (β2M-/-). Thymic single-cell suspensions were generated as described above. Thymocytes were resuspended in cRPMI and seeded at 4 x 10^6 cells per milliliter.

Generation of MHC-I KO and β2mKO DC 2.4 cells

DC 2.4 cells were obtained from UC Berkeley's Cell Culture Facility. DC 2.4 cells were transduced using the lentiCas9-Blast vector (Addgene plasmid # 52962; http://n2t.net/addgene:52962; RRID: Addgene_52962) and selected with 10 ug/mL of Blasticidin (AG Scientific #3513-03-9). Guide-RNA sequences targeting mouse β2m, Qa-1^b, H2-K^b, and H2-D^b were selected using CRISPick (portals.broadinstitute.org/gppx/crispick/public), and sequences are as follows: β2m: TCACGCCACCCACCGGAGAA, Qa-1^b: TACTACAATCAGAGTAACGA, H2-K^b: GTACATGGA AGTCGGCTACG, H2-D^b: AGATGTACCGGGGCTCCTCG. Guide-RNAs were stably transduced in SpCas9-expressing DC 2.4 cells using the LentiGuide-Neo vector and selected with 500 ug/mL of G418 (InvivoGen #108321-42-2). LentiGuide-Neo was a gift from Caroline Goujon (Addgene plasmid # 139449; http://n2t.net/addgene:139449; RRID: Addgene_139449). DC 2.4 cells that were negative for surface β2m, Qa-1^b, Qa-1^b x H2-D^b, Qa-1^b x H2-K^b, and Qa-1^b x H2-D^b x H2-K^b were independently sorted out on BD FACSAria Fusion (BD Biosciences).

In vitro stimulation with DC2.4 cells

WT, Qa1^{b}KO, Qa1^{b}K^{b}D^{b}KO, Qa1^{b}K^{b}KO, Qa1^{b}D^{b}KO, and β2mKO DC2.4 cells were plated in 48 Well Cell Culture Plates (Corning, Cat. No:3548) at 3x10^5 cells per well. Cells were left to settle for 1 hour at 37°C 5% CO_2. DC2.4 cells were then treated with 5ng/ml Recombinant Mouse IFN-γ (Biolegend, Cat. No:575302) for 24 hours, then Recombinant Mouse IFN-γ was washed off. Single-cell suspensions of QFLTgβ2mKO thymi were prepared as described above. Thymocytes were overlaid at 1x10^5 cells per well and cultured at 37°C 5% CO_2 for 24 hours, then harvested for flow cytometric analyses.

Thymic tissue slice cultures

Thymic lobes from wild type, Qa1^{b}KO and β2mKO mice were gently isolated and any connective tissue was removed. Lobes were embedded into 4% agarose with a low melting point (GTG-NuSieve Agarose, Lonza) and sectioned into 400-500mm slices using a vibratome (VT1000S, Leica). Thymic slices were overlaid onto 0.4mm transwell inserts (Corning, Cat. No.: 353090) in 6 well tissue culture plates with enough cRPMI under the insert to reach the slices. Pre-selection QFL (2.5x10^5) thymocytes were overlaid onto each slice and allowed to migrate for 3 hours, after which excess thymocytes were removed by gently washing with PBS. Slices were cultured at 37°C 5% CO2 until harvested for analysis. For flow cytometry, thymic slices were mechanically dissociated into single-cell suspensions prior to staining.

Bone marrow chimeras

Host mice were depleted of NK cells by I.P. injecting anti-NK1.1 (PK136, Leinco Technologies, #N123) at 100ug/100uL every 24Hrs for two days, for a total of 200ug of depleting antibody. Mice were irradiated in two doses of 600 rads (total of 1,200rads), with a resting period of 16hrs between doses. Mice were maintained on antibiotic water (Trimethoprim/Sulfamethoxazole) 4 weeks following irradiation. Bone marrow was harvested from the femur of donor mice using standard techniques. Red blood cells were lysed using ACK lysis buffer (0.15M NH4Cl, 1mM KHCO3, 0.1mM Na2EDTA) for 5 minutes at room temperature. Cells were depleted of CD4+ T cells by staining with CD4 PE-conjugated antibody (RM4-4) for 20 minutes at 4°C and then with Anti-PE MicroBeads (Miltenyi Biotec.) as described above. The labeled cells were washed, resuspended in MACS buffer, and then passed through a magnetic column (Miltenyi Biotec.). Flow-through (CD4-depleted bone marrow cells) was washed, resuspended at (4x10^6 cells) in 100uL of PBS and i.v. injected into recipient mice. Bone marrow chimeras were analyzed 8-11 weeks following reconstitution.

CFSE labeling

Cells were resuspended in 5uM CFSE proliferation dye (ThermoFisher #C34554) and incubated at 37°C for 9 minutes. Cells were then washed by addition of pre-warmed cRPMI while vortexing. Cells were then washed again with pre-warmed PBS and resuspended at the desired concentration.

In vitro stimulation with splenocytes

Single cell-suspensions of splenocytes were generated and RBC lysed as described above. Antigen presenting cells (APCs) were prepared by depleting splenocytes of CD4, CD8, and NK1.1 expressing cells using a magnetic column as described above. APCs were seeded at 4x10^5 cells per well in a 48 well plates. Responding cells were splenocytes from QFLTg mice that were depleted of CD4, NK1.1, B220, and CD19 expressing cells using a magnetic column as described above. Cells were then CFSE (ThermoFisher #C34554) labeled as described above and seeded at 1x10^5 cells per well.

Generation of RAG2KO neonatal chimera

Donor thymocytes and splenocytes were isolated as described above. Single cell suspensions were depleted of CD4+ T cells, B cells and NK cells by staining with CD4 (RM4-4), CD19 (1D3), and NK1.1(PK136) PE-conjugated antibody for 20 minutes at 4°C and then with Anti-PE MicroBeads (Miltenyi Biotec) as described above. The labeled cells were washed, resuspended in cRPMI

buffer, and then passed through a magnetic column (Miltenyi Biotec). Flow-through (CD4, CD19, NK1.1 depleted cells) was washed, resuspended at ($1x10^6$ cells) in 100uL of PBS and intrahepatically injected into 4–6-day old Rag2KO recipients. Recipient mice were analyzed 14-15 weeks post-injection.

Data availability statement

The original contributions presented in the study are included in the article/Supplementary Material. Further inquiries can be directed to the corresponding author.

Ethics statement

The animal study was approved by Institutional Animal Care and Use Committee. The study was conducted in accordance with the local legislation and institutional requirements.

Author contributions

MV and KA performed experiments and data analysis and contributed equally to this work and share the first authorship. JG, SC, XY, NK, and AL assisted in the generation of models and methods utilized in this publication, as well as advised on the progress of the study. NS and LC provided guidance in the writing and designing of this publication. ER is the senior author of this publication providing mentorship to the first authors and leading the design and writing of this publication. All authors contributed to the article and approved the submitted version.

Funding

Funding was provided by the National Institutes of Health (RO1AI149341). MM was supported by a National Science Foundation Graduate Research Fellowship and a diversity supplement to R01AI149341.

Acknowledgments

We thank Kartoosh Heydari, H. Nolla, and A. Valero of the UC Berkeley Cancer Research Lab for help with flow cytometry. We thank members of the Shastri, Coscoy, Raulet, and Robey lab for helpful discussions.

Conflict of interest

The authors declare that the research was conducted in the absence of any commercial or financial relationships that could be construed as a potential conflict of interest.

Publisher's note

Supplementary material

The Supplementary Material for this article can be found online at: https://www.frontiersin.org/articles/10.3389/fimmu.2023.1250316/full#supplementary-material

SUPPLEMENTARY FIGURE 1
Gating Strategy utilized to identify QFL T cells in distinct tissues. **(A)** Representative gating strategy employed to identify QFL CD8SP T cells in non-transgenic (tetramer enriched) and QFLTg thymocytes. Note that virtually all QFL tetramer$^+$CD24$^-$ from QFLTg mice express Vα3.2 (lower histogram). **(B)** Representative plots showing the gating strategy to identify QFL CD8SP T cells in non-transgenic (tetramer enriched) and QFLTg spleen and IEL compartment of the small intestine. Example shown from Spleen of non-transgenic mice. **(C)** Representative flow plots illustrating gates identifying CD8αβ and CD8α$^+$βlow populations within CD8SP T cells in the IEL compartment (Left) Total CD8SP T cells (Gated: B220$^-$ TCRβ$^+$CD8α$^+$CD4$^-$) (Right) QFL CD8SP T cells (Gated: B220$^-$TCRβ$^+$QFL tetramer$^+$Vα3.2$^+$CD8α$^+$CD4$^-$) **(D, E)** (Left) Representative plots of CD8α and CD8β on QFL CD8SP splenocytes (Middle) Representative plots CD4, CD8α and CD8β of QFL T cells in the SI IEL compartment. (Right) Compiled data showing the % of indicated populations in QFL IEL compartment (Gated: TCRβ$^+$QFL tetramer$^+$Vα3.2$^+$) **(D)** (n=10) and QFLTg **(E)** (n=5) mice. CD4SP (CD4$^+$CD8α$^-$) (Black dots), DN (CD4-CD8α$^-$) (Magenta dots), CD8αα(CD4$^-$CD8α$^+$CD8β$^-$) (Teal dots), CD8αβ (CD4$^-$CD8α$^+$CD8β$^+$) (Purple dots). Error bars= Standard error of mean. Statistical Analysis: One way ANOVA followed by Tukey's multiple comparison test was used to compare each sample to each other (P values are *<0.05,**<0.005, ***<0.0005. Comparisons that are not statistically significant are not marked by a symbol.

SUPPLEMENTARY FIGURE 2
Characterization of QFL TCR transgenic mice. **(A)** Representative flow plots of CD4 and CD8α expression on thymocytes from QFLTg mice (Gated: Live) or Vα3.2 and CD24 expression of indicated thymocyte populations. Data from wild type mice is show below for comparison. **(B)** Representative flow plots of Vα2 and Vα3.2 expression in CD8SP (Gated: CD8α$^+$CD4$^-$CD24$^-$) and CD4SP (Gated: CD8α$^-$CD4$^+$CD24$^-$) thymocytes from QFLTg and WT mice. Central dot plots show compiled data of Vα2 expression on SP thymocytes from QFLTg (n=4) and WT (n=3) mice. Right most plots show compiled data of Vα2 expression out of QFL CD8SP (Gated: QFL tetramer$^+$CD24$^-$CD8α$^+$CD4$^-$) thymocytes from QFLTg (n=4) and QFLTgQa1^{b}KO (n=4) mice. Dotted line indicates average value for mature CD8SP thymocytes from wild type mice. Each dot represents an individual mouse. **(C)** Representative flow plots of Vα2 and Vα3.2 expression in CD8SP and CD4SP splenocytes from QFLTg and WT mice. Central dot plots show compiled data of Vα2 expression on SP splenocytes from QFLTg (n=4) and WT (n=3) mice [Gated: TCRβ$^+$B220$^-$ CD8α$^+$CD4$^-$ (CD8SP) or TCRβ$^+$B220$^-$CD8α$^+$CD4$^-$ (CD4SP)]. Right most plots show compiled data of Vα2 expression out of QFL CD8SP (Gated: TCRβ$^+$B220$^-$QFL tetramer$^+$CD8α$^+$CD4$^-$) splenocytes from QFLTg (n=4) and QFLTgQa1^{b}KO (n=4) mice. Dotted line indicates average value for mature CD8SP splenocytes from wild type mice. Each dot represents an individual mouse. **(D)** Representative flow plots of (Top) QFL tetramer and QDM tetramer and (Bottom) NKG2A and QDM tetramer on QFLTg thymocytes (Gated: QFL tetramer$^+$CD24$^-$) and QFLTg splenocytes (Gated: TCRβ$^+$B220$^-$ QFL tetramer$^+$). Error bars= Standard error of mean. Statistical analysis: Two-way ANOVA followed by Tukey's multiple comparison test comparing experimental samples to each other in their respective genetic background

(B, C). Student's t test comparing QFLTg and QFLTgQa1^{b}KO samples to each other **(B, C)**. P values are * <0.05, ** <0.005, ***<0.0005. Comparisons that are not statistically significant are not marked by a symbol.

SUPPLEMENTARY FIGURE 3

Characterization of QFL CD8SP thymocytes. **(A)** Representative histograms of PLZF (n=6), Tbet (n=4), PD1 (n=5), α4β7(n=4) and CD44 (n=6) expression in QFL CD8SP thymocytes (Light Blue curve/dots) (Gated: QFL tetramer^{+}CD24^{-} CD8α+CD4^{-}). Conventional CD8SP thymocytes (Grey histogram/dots) (Gated: CD8α^{+}CD4^{-}) are shown for comparison. **(B)** Percentage of PLZF^{+} out of QFL CD8SP thymocytes or conventional CD8SP (Conv CD8SP) thymocytes. **(C)** gMFI of Tbet, PD1, α4β7 and CD44 of QFL CD8SP thymocytes normalized to the gMFI of conventional CD8SP thymocytes (Dotted line). Error bars= Standard error of mean. Statistical analysis: Student's t test was used to compare experimental samples to each other **(B)**. One-sample t test was used to compare experimental samples to the control used for normalization **(C)**: shown below experimental label. P values are * <0.05, **<0.005, ***<0.0005. Comparisons that are not statistically significant are not marked by a symbol.

SUPPLEMENTARY FIGURE 4

Phenotype of K^{b}D^{b}KO and Qa1^{b}KO thymus and spleen. **(A)** Representative flow plots of CD4 and CD8α expression of unenriched WT, K^{b}D^{b}KO, Qa1^{b}KO and β2mKO thymocytes (Gated: Live cells) and splenocytes (Gated: TCRβ^{+}). **(B)** Representative flow plots of QFL tetramer and Vα3.2 TCR expression on tetramer enriched thymocytes (Gated: Live) and splenocytes (Gated: TCRβ^{+}) of B6, K^{b}D^{b}KO, Qa1^{b}KO and β2mKO mice. **(C)** Number of QFL T cells in thymi (tetramer enriched and gated: QFL tetramer^{+}Vα3.2^{+}CD8α^{+}CD4^{-}) or spleen (tetramer enriched and gated: TCRβ^{+}QFL tetramer^{+}Vα3.2^{+} CD8α^{+}CD4^{-}) of non-transgenic mice of the indicated genotype. Thymus (WT (purple) n=9, K^{b}KO (magenta) n=4, D^{b}KO (black) n=4 K^{b}D^{b}KO (teal) n=4) Spleen (WT n=8, K^{b}KO=5, D^{b}KO=5 K^{b}D^{b}KO n=4). **(D)** Frequency of Vα3.2+ cells out of CD8SP splenocytes (Gated: TCRβ^{+}B220^{-}CD8α^{+}CD4^{-}) from the indicated mouse strains (WT (purple) n=16, Qa1^{b}KO (magenta) n=8, K^{b}D^{b}KO (teal) n=10). **(E)** Representative histogram and compiled data of CD44 expression on QFLCD8SP T cells (Gated: TCRβ^{+}QFL tetramer^{+}Vα3.2^{+}CD8α^{+}) in Non-Transgenic (WT (purple) n=32, Qa1^{b}KO magenta) n=8 and K^{b}D^{b}KO (teal) n=9), QFL Transgenic(WT n=11, Qa1^{b}KO n=6 and K^{b}D^{b}KO n=7) and conventional CD8SP (conv CD8SP, black) (n=10) (Gated: TCRβ^{+}CD8α^{+}CD4^{-}) from unenriched non-transgenic spleens. Error bars= Standard error of mean. Statistical analyses: One way ANOVA followed by Tukey's multiple comparison test comparing each experimental sample to each other **(C–E)**. P values are *<0.05, **<0.005, ***<0.0005. Comparisons that are not statistically significant are not marked by a symbol.

SUPPLEMENTARY FIGURE 5

QFL thymocyte stimulation *in-vitro*. **(A)** Representative flow cytometry plots of CD5 and CD69 expression on preQFLTg thymocytes (from QFLTg β2mKO mice) (Gated: QFL tetramer^{+}Vα3.2^{+}CD4^{+}CD8α^{+}) after 24 hours of co-culture with Bone Marrow Derived Dendritic cells (BMDC) from the indicated mouse strains. **(B, C)** PreQFLTg thymocytes were overlaid onto thymic tissue slices from the indicated mouse strains. Representative flow cytometry plots of **(B)** CD5 and CD69 expression or **(C)** CD5 and CD4 expression on QFL DP thymocytes (Gated: QFL tetramer^{+}Vα3.2^{+}CD4^{+}CD8α^{+}) after 3 (n=5 for all conditions) and 24 (n=5 for all conditions) hours of co-culture. Dot plots show compiled data of two experiments, with each dot representing a sample from an individual thymic slice. **(D)** Representative flow cytometry plots of CD5 and CD69 expression on preQFLTg DP thymocytes that were co-cultured for 24Hrs with either parental (WT) DC2.4 cells or DC2.4 cells in which genes encoding the indicated MHC molecules were knocked out using CRISPR/Cas9 editing (Gated: QFL tetramer^{+}Vα3.2^{+}CD4^{+}CD8α^{+}). Error bars= Standard error of mean. Statistical analysis: Two-way ANOVA followed by Tukey's multiple comparison test comparing samples to each other in their respective time point **(B, C)**. P values are *<0.05, ** <0.005, ***<0.0005. Comparisons that are not statistically significant are not marked by a symbol.

SUPPLEMENTARY FIGURE 6

Requirement for hematopoietic cells versus non-hematopoietic cell MHC I expression in QFL T cell development in non-transgenic mice. **(A)** Diagram of experimental design. Non-transgenic WT or β2mKO mice were used as bone marrow donors to reconstitute irradiated β2mKO or wild type hosts in order to restrict MHC I expression to hematopoietic or non-hematopoietic cells. **(B, C)** Absolute numbers of QFL CD8SP T cells in **(B)** thymus (tetramer enriched and gated: QFL tetramer^{+}Vα3.2^{+}CD8α^{+}) and **(C)** spleens (tetramer enriched and gated: TCRβ^{+}QFL tetramer^{+}Vα3.2^{+}CD8α^{+}) from the indicated chimeric mice. WT>β2mKO (black dots, n=3), β2mKO>WT (magenta dots, n=3) and WT>WT (teal dots, n=5). **(D)** Downregulation of CD8β of QFL CD8SP thymocytes of the indicated chimeric mice (WT>β2mKO (black) n=10, β2mKO>WT (magenta) n=10, WT>WT (teal) n=5). Conventional CD8SP (Conv CD8SP) (light blue, n=3) (Gated: CD8α^{+}CD4^{-}) from unenriched non-transgenic mice shown for comparison. **(E)** Relative CD5 expression on QFL CD8SP thymocytes of the indicated chimeric mice. Graph shows gMFI of CD5 expression of QFL thymocytes normalized to the gMFI for conventional CD8SP (conv CD8SP) analyzed in the same experiment (WT>β2mKO n=3, β2mKO>WT n=3, WT>WT n=6). **(F)** Quantification of CD44 expression of QFL CD8SP T cells (Gated: TCRβ^{+}QFL tetramer^{+}Vα3.2^{+}CD8α^{+}CD4^{-}) from tetramer enriched non-transgenic splenocytes from: WT>β2mKO (n=3), β2mKO>WT(n=3), WT>WT (n=3) chimeric spleens. For comparison conventional CD8SP (Conv CD8SP) (light blue) (n=3) (Gated: TCRβ^{+}CD8α^{+}) from unenriched non-transgenic mice. Error bars= Standard error of mean. Statistical analysis: One way ANOVA followed by Tukey's multiple comparison test comparing each experimental sample to each other **(B–F)**; shown above dots. One-sample t test was used to compare experimental samples to the control used for normalization **(E)**; shown below label. P values are * <0.05, **<0.005, ***<0.0005. Comparisons that are not statistically significant are not marked by a symbol.

References

1. Legoux F, Salou M, Lantz O. Unconventional or preset αβ T cells: evolutionarily conserved tissue-resident T cells recognizing nonpeptidic ligands. *Annu Rev Cell Dev Biol* (2017) 33(1):511–35. doi: 10.1146/annurev-cellbio-100616-060725

2. Rodgers JR, Cook RG. MHC class Ib molecules bridge innate and acquired immunity. *Nat Rev Immunol* (2005) 5(6):459–71. doi: 10.1038/nri1635

3. Adams EJ, Luoma AM. The adaptable major histocompatibility complex (MHC) fold: structure and function of nonclassical and MHC class I-like molecules. *Annu Rev Immunol* (2013) 31(1):529–61. doi: 10.1146/annurev-immunol-032712-095912

4. Seach N, Guerri L, le Bourhis L, Mburu Y, Cui Y, Bessoles S, et al. Double-positive thymocytes select mucosal-associated invariant T cells. *J Immunol* (2013) 191 (12):6002–9. doi: 10.4049/jimmunol.1301212

5. Bendelac A. Positive selection of mouse NK1+ T cells by CD1-expressing cortical thymocytes. *J Exp Med* (1995) 182(6):2091–6. doi: 10.1084/jem.182.6.2091

6. Stritesky GL, Jameson SC, Hogquist KA. Selection of self-reactive T cells in the thymus. *Annu Rev Immunol* (2012) 30:95–114. doi: 10.1146/annurev-immunol-020711-075035

7. Berg RE, Princiotta MF, Irion S, Moticka JA, Dahl KR, Staerz UD. Positive selection of an H2-M3 restricted T cell receptor. *Immunity* (1999) 11(1):33–43. doi: 10.1016/S1074-7613(00)80079-5

8. Cho H, Bediako Y, Xu H, Choi HJ, Wang CR. Positive selecting cell type determines the phenotype of MHC class Ib-restricted CD8+ T cells. *Proc Natl Acad Sci USA* (2011) 108(32):13241–6. doi: 10.1073/pnas.1105118108

9. Sullivan BA, Kraj P, Weber DA, Ignatowicz L, Jensen PE. Positive selection of a Qa-1-restricted T cell receptor with specificity for insulin. *Immunity* (2002) 17(1):95–105. doi: 10.1016/S1074-7613(02)00343-6

10. Doorduijn EM, Sluijter M, Querido BJ, Oliveira CC, Achour A, Ossendorp F, et al. TAP-independent self-peptides enhance T cell recognition of immune-escaped tumors. *J Clin Invest* (2016) 126(2):784–94. doi: 10.1172/JCI83671

11. Bediako Y, Bian Y, Zhang H, Cho H, Stein PL, Wang CR. SAP is required for the development of innate phenotype in H2-M3–restricted Cd8(+) T cells. *J Immunol* (2012) 189(10):4787–96. doi: 10.4049/jimmunol.1200579

12. Chiu NM, Wang B, Kerksiek KM, Kurlander R, Pamer EG, Wang CR. The selection of M3-restricted T cells is dependent on M3 expression and presentation of N-formylated peptides in the thymus. *J Exp Med* (1999) 190(12):1869–78. doi: 10.1084/jem.190.12.1869

13. Park SH, Guy-Grand D, Lemonnier FA, Wang CR, Bendelac A, Jabri B. Selection and expansion of CD8alpha/alpha(1) T cell receptor alpha/beta(1) intestinal intraepithelial lymphocytes in the absence of both classical major histocompatibility

complex class I and nonclassical CD1 molecules. *J Exp Med* (1999) 190(6):885–90. doi: 10.1084/jem.190.6.885

14. Gapin L, Cheroutre H, Kronenberg M. Cutting edge: TCR alpha beta+ CD8 alpha alpha+ T cells are found in intestinal intraepithelial lymphocytes of mice that lack classical MHC class I molecules. *J Immunol* (1999) 163(8):4100–4. doi: 10.4049/jimmunol.163.8.4100

15. Das G, Gould DS, Augustine MM, Fragoso G, Sciutto E, Stroynowski I, et al. Qa-2-dependent selection of CD8alpha/alpha T cell receptor alpha/beta(+) cells in murine intestinal intraepithelial lymphocytes. *J Exp Med [Internet]* (2000) 192(10):1521–8. doi: 10.1084/jem.192.10.1521

16. Cheroutre H, Lambolez F, Mucida D. The light and dark sides of intestinal intraepithelial lymphocytes. *Nat Rev Immunol* (2011) 11(7):445–56. doi: 10.1038/nri3007

17. McDonald BD, Jabri B, Bendelac A. Diverse developmental pathways of intestinal intraepithelial lymphocytes. *Nat Rev Immunol* (2018) 18(8):514–25. doi: 10.1038/s41577-018-0013-7

18. Mayans S, Stepniak D, Palida S, Larange A, Dreux J, Arlian B, et al. αβT cell receptors expressed by CD4(-)CD8αβ(-) intraepithelial T cells drive their fate into a unique lineage with unusual MHC reactivities. *Immunity* (2014) 41(2):207–18. doi: 10.1016/j.immuni.2014.07.010

19. McDonald BD, Bunker JJ, Ishizuka IE, Jabri B, Bendelac A. Elevated T cell receptor signaling identifies a thymic precursor to the TCRαβ(+)CD4(-)CD8β(-) intraepithelial lymphocyte lineage. *Immunity* (2014) 41(2):219–29. doi: 10.1016/j.immuni.2014.07.008

20. Joannou K, Baldwin TA. Destined for the intestine - thymic selection of TCRαβ CD8αα intestinal intraepithelial lymphocytes. *Clin Exp Immunol* (2023) 213:1–9.

21. Pobezinsky LA, Angelov GS, Tai X, Jeurling S, van Laethem F, Feigenbaum L, et al. Clonal deletion and the fate of autoreactive thymocytes that survive negative selection. *Nat Immunol* (2012) 13(6):569–78. doi: 10.1038/ni.2292

22. Ruscher R, Kummer RL, Lee YJ, Jameson SC, Hogquist KA. CD8αα intraepithelial lymphocytes arise from two main thymic precursors. *Nat Immunol* (2017) 18(7):771–9. doi: 10.1038/ni.3751

23. Klose CSN, Hummel JF, Faller L, D'Hargues Y, Ebert K, Tanriver Y. A committed postselection precursor to natural TCRαβ+ intraepithelial lymphocytes. *Mucosal Immunol* (2018) 11(2):333–44. doi: 10.1038/mi.2017.54

24. Golec DP, Hoeppli RE, Caviedes LMH, McCann J, Levings MK, Baldwin TA. Thymic progenitors of TCRαβ+ CD8αα intestinal intraepithelial lymphocytes require RasGRP1 for development. *J Exp Med* (2017) 214(8):2421–36. doi: 10.1084/jem.20170844

25. Klose CSN, Blatz K, D'Hargues Y, Hernandez PP, Kofoed-Nielsen M, Ripka JF, et al. The transcription factor T-bet is induced by IL-15 and thymic agonist selection and controls CD8αα(+) intraepithelial lymphocyte development. *Immunity* (2014) 41(2):230–43. doi: 10.1016/j.immuni.2014.06.018

26. Sharpe HR, Bowyer G, Brackenridge S, Lambe T. HLA-E: exploiting pathogen-host interactions for vaccine development. *Clin Exp Immunol* (2019) 196(2):167–77. doi: 10.1111/cei.13292

27. van Hall T, Oliveira CC, Joosten SA, Ottenhoff THM. The other Janus face of Qa-1 and HLA-E: diverse peptide repertoires in times of stress. *Microbes Infect* (2010) 12(12–13):910–8. doi: 10.1016/j.micinf.2010.07.011

28. Vance RE, Kraft JR, Altman JD, Jensen PE, Raulet DH. Mouse CD94/NKG2A is a natural killer cell receptor for the nonclassical major histocompatibility complex (MHC) class I molecule Qa-1(b). *J Exp Med* (1998) 188(10):1841–8. doi: 10.1084/jem.188.10.1841

29. Braud VM, Allan DSJ, O'Callaghan CA, Söderström K, D'Andrea A, Ogg GS, et al. HLA-E binds to natural killer cell receptors CD94/NKG2A, B and C. *Nature* (1998) 391(6669):795–9. doi: 10.1038/35869

30. Hammer GE, Gonzalez F, James E, Nolla H, Shastri N. In the absence of aminopeptidase ERAAP, MHC class I molecules present many unstable and highly immunogenic peptides. *Nat Immunol* (2007) 8(1):101–8. doi: 10.1038/ni1409

31. Nagarajan NA, Gonzalez F, Shastri N. Nonclassical MHC class Ib-restricted cytotoxic T cells monitor antigen processing in the endoplasmic reticulum. *Nat Immunol* (2012) 13(6):579–86. doi: 10.1038/ni.2282

32. Doorduijn EM, Sluijter M, Querido BJ, Seidel UJE, Oliveira CC, van der Burg SH, et al. T cells engaging the conserved MHC class Ib molecule Qa-1b with TAP-independent peptides are semi-invariant lymphocytes. *Front Immunol* (2018) 9:60/full (January). doi: 10.3389/fimmu.2018.00060/full

33. Geiger KM, Manoharan M, Coombs R, Park C, AY L, Shastri N, et al. Murine cytomegalovirus downregulates ERAAP and induces an unconventional T cell response to self. *bioRxiv* (2022) 9. doi: 10.1101/2022.08.23.504566

34. Anderson CK, Reilly EC, Lee AY, Brossay L. Qa-1-restricted CD8+ T cells can compensate for the absence of conventional T cells during viral infection. *Cell Rep [Internet].* (2019) 27(2):537–548.e5. doi: 10.1016/j.celrep.2019.03.059

35. Caccamo N, Sullivan LC, Brooks AG, Dieli F. Harnessing HLA-E-restricted CD8 T lymphocytes for adoptive cell therapy of patients with severe COVID-19. *Br J Haematol [Internet]* (2020) 190(4):e185–7. doi: 10.1371/journal.ppat.1006384

36. Seaman MS, Perarnau B, Lindahl KF, Lemonnier FA, Forman J. Response to Listeria monocytogenes in mice lacking MHC class Ia molecules. *J Immunol* (1999) 162(9):5429–36. doi: 10.4049/jimmunol.162.9.5429

37. Shang S, Siddiqui S, Bian Y, Zhao J, Wang CR. Nonclassical MHC Ib-restricted CD8+ T cells recognize mycobacterium tuberculosis-derived protein antigens and contribute to protection against infection. *PloS Pathog* (2016) 12(6):e1005688. doi: 10.1371/journal.ppat.1005688

38. Lo WF, Ong H, Metcalf ES, Soloski MJ. T cell responses to Gram-negative intracellular bacterial pathogens: a role for CD8+ T cells in immunity to Salmonella infection and the involvement of MHC class Ib molecules. *J Immunol* (1999) 162(9):5398–406. doi: 10.4049/jimmunol.162.9.5398

39. Hansen SG, Wu HL, Burwitz BJ, Hughes CM, Hammond KB, Ventura AB, et al. Broadly targeted $CD8^+$ T cell responses restricted by major histocompatibility complex E. *Science* (2016) 351(6274):714–20. doi: 10.1126/science.aac9475

40. Yang H, Rei M, Brackenridge S, Brenna E, Sun H, Abdulhaqq S, et al. HLA-E-restricted, Gag-specific CD8+ T cells can suppress HIV-1 infection, offering vaccine opportunities. *Sci Immunol* (2021) 6(57):1–12. doi: 10.1126/sciimmunol.abg1703

41. Guan J, Yang SJ, Gonzalez F, Yin Y, Shastri N. Antigen processing in the endoplasmic reticulum is monitored by semi-invariant αβ TCRs specific for a conserved peptide-qa-1b MHC class Ib ligand. *J Immunol* (2017) 198(5):2017–27. doi: 10.4049/jimmunol.1600764

42. White JT, Cross EW, Kedl RM. Antigen-inexperienced memory CD8+ T cells: where they come from and why we need them. *Nat Rev Immunol* (2017) 17(6):391–400. doi: 10.1038/nri.2017.34

43. Jameson SC, Masopust D. Understanding subset diversity in T cell memory. *Immunity* (2018) 48(2):214–26. doi: 10.1016/j.immuni.2018.02.010

44. Obar JJ, Khanna KM, Lefrançois L. Endogenous naive CD8+ T cell precursor frequency regulates primary and memory responses to infection. *Immunity* (2008) 28(6):859–69. doi: 10.1016/j.immuni.2008.04.010

45. Mandl JN, Monteiro JP, Vrisekoop N, Germain RN. T cell-positive selection uses self-ligand binding strength to optimize repertoire recognition of foreign antigens. *Immunity* (2013) 38(2):263–74. doi: 10.1016/j.immuni.2012.09.011

46. Fulton RB, Hamilton SE, Xing Y, Best JA, Goldrath AW, Hogquist KA, et al. The TCR's sensitivity to self peptide-MHC dictates the ability of naive CD8(+) T cells to respond to foreign antigens. *Nat Immunol* (2015) 16(1):107–17. doi: 10.1038/ni.3043

47. Azzam HS, DeJarnette JB, Huang K, Emmons R, Park CS, Sommers CL, et al. Fine tuning of TCR signaling by CD5. *J Immunol* (2001) 166(9):5464–72. doi: 10.4049/jimmunol.166.9.5464

48. Persaud SP, Parker CR, Lo WL, Weber KS, Allen PM. Intrinsic CD4+ T cell sensitivity and response to a pathogen are set and sustained by avidity for thymic and peripheral complexes of self peptide and MHC. *Nat Immunol* (2014) 15(3):266–74. doi: 10.1038/ni.2822

49. Kurd NS, Hoover A, Yoon J, Weist BM, Lutes L, Chan SW, et al. Factors that influence the thymic selection of CD8αα intraepithelial lymphocytes. *Mucosal Immunol* (2021) 14(1):68–79. doi: 10.1038/s41385-020-0295-5

50. Yamagata T, Mathis D, Benoist C. Self-reactivity in thymic double-positive cells commits cells to a CD8 alpha alpha lineage with characteristics of innate immune cells. *Nat Immunol* (2004) 5(6):597–605. doi: 10.1038/ni1070

51. Savage AK, Constantinides MG, Han J, Picard D, Martin E, Li B, et al. The transcription factor PLZF directs the effector program of the NKT cell lineage. *Immun [Internet].* (2008) 29(3):391–403. doi: 10.1016/j.immuni.2008.07.011

52. Koay HF, Gherardin NA, Enders A, Loh L, Mackay LK, Almeida CF, et al. A three-stage intrathymic development pathway for the mucosal-associated invariant T cell lineage. *Nat Immunol* (2016) 17(11):1300–11. doi: 10.1038/ni.3565

53. Robinson PJ, Travers PJ, Stackpoole A, Flaherty L, Djaballah H. Maturation of Qa-1b class I molecules requires beta 2-microglobulin but is TAP independent. *J Immunol* (1998) 160(7):3217–24. doi: 10.4049/jimmunol.160.7.3217

54. Lee ST, Georgiev H, Breed ER, Ruscher R, Hogquist KA. MHC Class I on murine hematopoietic APC selects Type A IEL precursors in the thymus. *Eur J Immunol* (2021) 51(5):1080–8. doi: 10.1002/eji.202048996

55. Kreslavsky T, Kim HJ, Koralov SB, Ghitza D, Buch T, Cantor H, et al. Negative selection, not receptor editing, is a physiological response of autoreactive thymocytes. *J Exp Med* (2013) 210(10):1911–8. doi: 10.1084/jem.20130876

56. McDonald BD, Bunker JJ, Erickson SA, Oh-Hora M, Bendelac A. Crossreactive αβ T cell receptors are the predominant targets of thymocyte negative selection. *Immunity* (2015) 43(5):859–69. doi: 10.1016/j.immuni.2015.09.009

57. Lucas B, Stefanová I, Yasutomo K, Dautigny N, Germain RN. Divergent changes in the sensitivity of maturing T cells to structurally related ligands underlies formation of a useful T cell repertoire. *Immunity* (1999) 10(3):367–76. doi: 10.1016/S1074-7613(00)80036-9

58. Davey GM, Schober SL, Endrizzi BT, Dutcher AK, Jameson SC, Hogquist KA. Preselection thymocytes are more sensitive to T cell receptor stimulation than mature T cells. *J Exp Med* (1998) 188(10):1867–74. doi: 10.1084/jem.188.10.1867

59. Golec DP, Hoeppli RE, Henao Caviedes LM, McCann J, Levings MK, Baldwin TA. Thymic progenitors of TCRαβ+ CD8αα intestinal intraepithelial lymphocytes require RasGRP1 for development. *J Exp Med* (2017) 214(8):2421–35. doi: 10.1084/jem.20170844

60. Reed-Loisel LM, Sullivan BA, Laur O, Jensen PE. An MHC class Ib-restricted TCR that cross-reacts with an MHC class Ia molecule. *J Immunol* (2005) 174(12):7746–52. doi: 10.4049/jimmunol.174.12.7746

61. Li Y, Mathis A, Grewe BF, Osterhout JA, Ahanonu B, Schnitzer MJ, et al. Neuronal representation of social information in the medial amygdala of awake behaving mice. *Cell* (2017) 171(5):1176–90. doi: 10.1016/j.cell.2017.10.015

62. Sim BC, Lo D, Gascoigne NRJ. Preferential expression of TCR V alpha regions in CD4/CD8 subsets: class discrimination or co-receptor recognition? *Immunol Today* (1998) 19(6):276–82. doi: 10.1016/S0167-5699(98)01257-2

63. Prasad M, Wojciech L, Brzostek J, Hu J, Chua YL, Tung DWH, et al. Expansion of an unusual virtual memory CD8+ Subpopulation bearing Vα3.2 TCR in themis-deficient mice. *Front Immunol* (2021) 12(April):644483.

64. Kambayashi T, Kraft-Leavy JR, Dauner JG, Sullivan BA, Laur O, Jensen PE. The nonclassical MHC class I molecule Qa-1 forms unstable peptide complexes. *J Immunol* (2004) 172(3):1661–9. doi: 10.4049/jimmunol.172.3.1661

65. Sullivan LC, Clements CS, Rossjohn J, Brooks AG. The major histocompatibility complex class Ib molecule HLA-E at the interface between innate and adaptive immunity. *Tissue Antigens* (2008) 72(5):415–24. doi: 10.1111/j.1399-0039.2008.01138.x

66. Grotzke JE, Harriff MJ, Siler AC, Nolt D, Delepine J, Lewinsohn DA, et al. The Mycobacterium tuberculosis phagosome is a HLA-I processing competent organelle. *PloS Pathog* (2009) 5(4):e1000374. doi: 10.1371/journal.ppat.1000374

67. Smith TRF, Tang X, Maricic I, Garcia Z, Fanchiang S, Kumar V. Dendritic cells use endocytic pathway for cross-priming class Ib MHC-restricted CD8αα + TCRαβ + T cells with regulatory properties. *J Immunol* (2009) 182(11):6959–68. doi: 10.4049/jimmunol.0900316

68. Zeng L, Sullivan LC, Vivian JP, Walpole NG, Harpur CM, Rossjohn J, et al. A structural basis for antigen presentation by the MHC class Ib molecule, Qa-1. *J Immunol* (2012) 188(1):302–10. doi: 10.4049/jimmunol.1102379

69. Braud V, Jones EY, McMichael A. The human major histocompatibility complex class Ib molecule HLA-E binds signal sequence-derived peptides with primary anchor residues at positions 2 and 9. *Eur J Immunol* (1997) 27(5):1164–9. doi: 10.1002/eji.1830270517

70. Hu D, Ikizawa K, Lu L, Sanchirico ME, Shinohara ML, Cantor H. Analysis of regulatory CD8 T cells in Qa-1-deficient mice. *Nat Immunol* (2004) 5(5):516–23. doi: 10.1038/ni1063

71. Kouskoff V, Signorelli K, Benoist C, Mathis D. Cassette vectors directing expression of T cell receptor genes in transgenic mice. *J Immunol Methods* (1995) 180(2):273–80. doi: 10.1016/0022-1759(95)00002-R

72. Chen S, Lee B, Lee AYF, Modzelewski AJ, He L. Highly efficient mouse genome editing by CRISPR ribonucleoprotein electroporation of zygotes. *J Biol Chem* (2016) 291(28):14457–67. doi: 10.1074/jbc.M116.733154

73. Lefrançois L, Lycke N. Isolation of mouse small intestinal intraepithelial lymphocytes, Peyer's patch, and lamina propria cells. *Curr Protoc Immunol* (2001), 1–16. doi: 10.1002/0471142735.im0319s17